Mechanistic and Theoretical Analysis of the Oxidative Addition of H_2 to Six-Coordinate Molybdenum and Tungsten Complexes $M(PMe_3)_4X_2$ (M = Mo, W; X = F, Cl, Br, I): An Inverse Equilibrium Isotope Effect and an Unprecedented Halide Dependence

Tony Hascall, Daniel Rabinovich, Vincent J. Murphy,† Michael D. Beachy, Richard A. Friesner,* and Gerard Parkin*

Contribution from the Department of Chemistry, Columbia University, New York, New York 10027

Received June 14, 1999

Abstract: Experimental observations, together with a theoretical analysis, indicate that the energetics of the oxidative addition of H_2 to the six-coordinate molybdenum and tungsten complexes *trans*-$M(PMe_3)_4X_2$ (M = Mo, W; X = F, Cl, Br, I) depend very strongly on the nature of both the metal and the halogen. Specifically, the exothermicity of the reaction increases in the sequences Mo < W and I < Br < Cl < F. Of most interest, this halogen dependence provides a striking contrast to that reported for oxidative addition of H_2 to the Vaska system, *trans*-$Ir(PPh_3)_2(CO)X$. A theoretical analysis suggests that the halide dependence for *trans*-$M(PMe_3)_4X_2$ is a result of both steric and electronic factors, the components of which serve to reinforce each other. Oxidative addition is thus favored sterically for the fluoride derivatives since the increased steric interactions upon forming the eight-coordinate complexes $M(PMe_3)_4H_2X_2$ would be minimized for the smallest halogen. The electronic component of the energetics is associated with the extent that π-donation from X raises the energy of the doubly occupied 3e*, π-antibonding, d_{xz} and d_{yz} pair of orbitals in *trans*-$M(PMe_3)_4X_2$. Consequently, with F as the strongest π-donor, *trans*-$M(PMe_3)_4X_2$ is destabilized with respect to $M(PMe_3)_4H_2X_2$ by $p_\pi-d_\pi$ interaction to the greatest extent for the fluoride complex, so that oxidative addition becomes most favored for this derivative. Equilibrium studies of the oxidative addition of H_2 to *trans*-$W(PMe_3)_4I_2$ have allowed the average W−H bond dissociation energy (BDE) in $W(PMe_3)_4H_2I_2$ to be determined [D(W−H) = 62.0(6) kcal mol^{-1}]. The corresponding average W−D BDE [D(W−D) = 63.8(7) kcal mol^{-1}] is substantially greater than the W−H BDE, to the extent that the oxidative addition reaction is characterized by an *inverse* equilibrium deuterium isotope effect [K_H/K_D = 0.63(5) at 60 °C]. The inverse nature of the equilibrium isotope effect is associated with the large number (six) of isotope-sensitive vibrational modes in the product, compared to the single isotope-sensitive vibrational mode in reactant H_2. A mechanistic study reveals that the latter reaction proceeds via initial dissociation of PMe_3, followed by oxidative addition to five-coordinate $[W(PMe_3)_3I_2]$, rather than direct oxidative addition to *trans*-$W(PMe_3)_4I_2$. Conversely, reductive elimination of H_2 does not occur directly from $W(PMe_3)_4H_2I_2$ but rather by a sequence that involves dissociation of PMe_3 and elimination from the seven-coordinate species $[W(PMe_3)_3H_2I_2]$.

Introduction

The oxidative addition of dihydrogen to a metal center and its microscopic reverse, reductive elimination, are two of the simplest yet most important transformations in organometallic chemistry.[1] For example, oxidative addition of dihydrogen is a key step in many, if not all, transition metal-catalyzed reactions involving H_2, as exemplified by olefin hydrogenation and hydroformylation.[2] In this paper, we describe a mechanistic and theoretical analysis of the oxidative addition of H_2 to the six-coordinate molybdenum and tungsten complexes $M(PMe_3)_4X_2$ (M = Mo, W; X = F, Cl, Br, I). This study demonstrates that the oxidative addition of dihydrogen is characterized by an *inverse* deuterium equilibrium isotope effect (i.e., $K_H/K_D < 1$) and also by a halide dependence (i.e., $K_F > K_{Cl} > K_{Br} > K_I$), which is counter to that in previously studied transition metal systems.[3]

Results and Discussion

We have recently reported the syntheses and molecular structures of the series of eight-coordinate tungsten hydride complexes $W(PMe_3)_4H_2X_2$ (X = F, Cl, Br, I).[4−6] Despite their similar structures, however, the stabilities of these complexes are markedly dependent upon the nature of the halogen. For

† Present address: Symyx Technologies, 3100 Central Expressway, Santa Clara, CA 95051.

(1) (a) Collman, J. P.; Hegedus, L. S.; Norton, J. R.; Finke, R. G. *Principles and Applications of Organotransition Metal Chemistry*; University Science Books: Mill Valley, CA, 1987. (b) Mondal, J. U.; Blake, D. M. *Coord. Chem. Rev.* **1982**, *47*, 205−238. (c) Hay, P. J. In *Transition Metal Hydrides*; Dedieu, A., Ed.; VCH: New York, 1992; pp 127−147.

(2) (a) Parshall, G. W.; Ittel, S. D. *Homogeneous Catalysis*, 2nd ed.; Wiley: New York, 1992. (b) James, B. R. In *Comprehensive Organometallic Chemistry*; Wilkinson, G., Stone, F. G. A., Abel, E. W., Eds.; Pergamon Press: New York, 1982; Vol. 8, Chapter 51, pp 285−363. (c) James, B. R. *Homogeneous Hydrogenation*; Wiley: New York, 1973.

(3) A portion of this work concerned with the equilibrium deuterium isotope effect has been communicated. See: Rabinovich, D.; Parkin, G. *J. Am. Chem. Soc.* **1993**, *115*, 353−354.

(4) Murphy, V. J.; Rabinovich, D.; Hascall, T.; Klooster, W. T.; Koetzle, T. F.; Parkin, G. *J. Am. Chem. Soc.* **1998**, *120*, 4372−4387.

10.1021/ja9920009 CCC: $18.00
Published on Web 11/30/1999

Table 1. Qualitative Thermal Stabilities of $M(PMe_3)_4H_2X_2$ Derivatives

	F	Cl	Br	I
Mo	$t_{1/2}$ > 2 days at 30 °C	$t_{1/2} \approx$ 2 h at 30 °C	$t_{1/2}$ < 30 min at 30 °C	not observed
W	stable at 60 °C	stable at 60 °C	stable at 60 °C	reversible elimination of H_2 at ambient temperature

example, whereas the fluoride, chloride,[7] and bromide derivatives are stable under ambient conditions, the iodide complex slowly reductively eliminates H_2 at ambient temperature to give *trans*-$W(PMe_3)_4I_2$.[8] The latter reaction is, however, reversible, and $W(PMe_3)_4I_2$ reacts with H_2 to give $W(PMe_3)_4H_2I_2$ (eq 1).

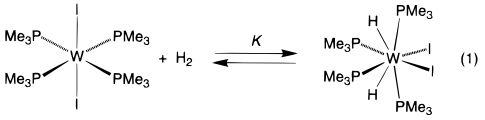

Together with the fact that $W(PMe_3)_4Cl_2$ reacts irreversibly with H_2 to give $W(PMe_3)_4H_2Cl_2$,[5b] these observations indicate that the W−H bond energies in the complexes $W(PMe_3)_4H_2X_2$ are strongly influenced by the nature of the halogen, being weakest for the iodide derivative. A similar trend is also observed in the molybdenum system, although the complexes $Mo(PMe_3)_4H_2X_2$ (X = F,[9] Cl, Br, I) are much less stable in solution than their tungsten counterparts (Table 1). Thus, while each of the complexes $Mo(PMe_3)_4H_2X_2$ may be generated by reaction of $Mo(PMe_3)_5H_2$ with HX,[10] only the fluoride complex $Mo(PMe_3)_4H_2F_2$[9] exhibits appreciable thermal stability: the chloro and bromo complexes $Mo(PMe_3)_4H_2X_2$ readily eliminate H_2 to give $Mo(PMe_3)_4X_2$,[11] while the iodo complex $Mo(PMe_3)_4H_2I_2$ is sufficiently unstable that it has not even been spectroscopically detected (Scheme 1).

The above observations clearly indicate that the thermodynamic ability of H_2 to oxidatively add to the metal center in $M(PMe_3)_4X_2$ is very dependent upon the nature of both the metal and the halogen. In view of the importance of oxidative addition and reductive elimination processes in organometallic chemistry,

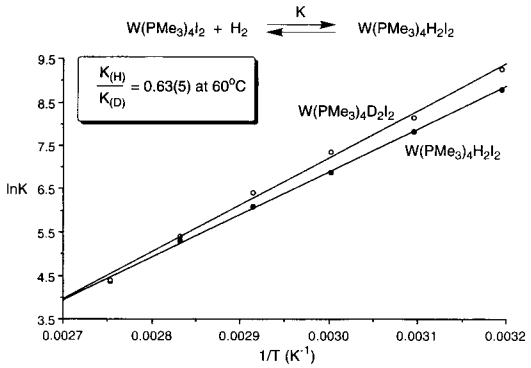

Figure 1. van't Hoff plots for oxidative addition of H_2 and D_2 to $W(PMe_3)_4I_2$.

Scheme 1. Syntheses and Reductive Elimination of $Mo(PMe_3)_4H_2X_2$

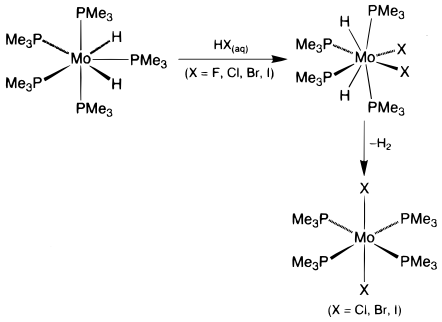

Table 2. Equilibrium Constants for the Oxidative Addition of H_2 (D_2) to $W(PMe_3)_4I_2$

T/°C	K_H/M^{-1}	K_D/M^{-1}	K_H/K_D
40	$6.6(7) \times 10^3$	$1.0(1) \times 10^4$	0.66(13)
50	$2.5(3) \times 10^3$	$3.5(4) \times 10^3$	0.71(14)
60	$1.0(1) \times 10^3$	$1.6(2) \times 10^3$	0.63(5)
70	$4.4(5) \times 10^2$	$6.0(6) \times 10^2$	0.73(15)
80	$2.0(2) \times 10^2$	$2.2(2) \times 10^2$	0.91(18)
90	$0.8(1) \times 10^2$	$0.8(1) \times 10^2$	1.00(20)

we have performed a combination of equilibrium, kinetics, and computational studies to ascertain the factors responsible for influencing these fundamental transformations.

Thermodynamics of Oxidative Addition of H_2: M−H Bond Dissociation Energies and the Origin of the Halide Dependence. (a) Equilibrium Studies. The magnitude of the equilibrium constant for oxidative addition of H_2 to the tungsten iodide complex *trans*-$W(PMe_3)_4I_2$ is such that, under 1 atm of H_2; the equilibrium constant can be determined by using ^{1}H NMR spectroscopy, and its temperature dependence (Figure 1 and Table 2) allows determination of the enthalpy and entropy for the oxidative addition: $\Delta H° = -19.7(6)$ kcal mol^{-1} and $\Delta S° = -45(2)$ eu[12] Since we may define $\Delta H° = D(H-H) -$

(5) For the first reports of the chloride derivative, $W(PMe_3)_4H_2Cl_2$, see: (a) Sharp, P. R. Ph.D. Thesis, Massachusetts Institute of Technology, 1980. (b) Sharp, P. R.; Frank, K. G. *Inorg. Chem.* **1985**, *24*, 1808−1813. (c) Chiu, K. W.; Lyons, D.; Wilkinson, G.; Thornton-Pett, M.; Hursthouse, M. B. *Polyhedron* **1983**, *2*, 803−810.

(6) For reviews on metal hydrides, see: (a) *Transition Metal Hydrides*; Dedieu, A., Ed.; VCH Publishers, Inc.: New York. 1991. (b) *Transition Metal Hydrides*; Muetterties, E. L., Ed.; Marcel Dekker, Inc.: New York, 1971. (c) Teller, R. G.; Bau, R. *Struct. Bonding (Berlin)* **1981**, *44*, 1−82. (d) Crabtree, R. H. In *Encyclopedia of Inorganic Chemistry*; King, R. B., Ed.; Wiley: New York, 1994; Vol. 3, pp 1392−1400. (e) Hlatky, G. G.; Crabtree, R. H. *Coord. Chem. Rev.* **1985**, *65*, 1−48. (f) Moore, D. S.; Robinson, S. D. *Chem. Soc. Rev.* **1983**, *12*, 415−452. (g) Kuhlman, R. *Coord. Chem. Rev.* **1997**, *167*, 205−232. (h) Also see the special volume: *Inorg. Chim. Acta* **1997**, *259*, Nos. 1 and 2.

(7) The thermal stability of $W(PMe_3)_4H_2Cl_2$ at 80 °C with respect to reductive elimination was first noted by Sharp (ref 5b).

(8) $W(PMe_3)_4I_2$ has also been reported to exist as a diamagnetic *cis*-isomer, but we have not observed such a species. See: Chiu, K. W.; Jones, R. A.; Wilkinson, G.; Galas, A. M. R.; Hursthouse, M. B.; Malik, K. M. A. *J. Chem. Soc., Dalton Trans.* **1981**, 1204−1211.

(9) Murphy, V. J.; Hascall, T.; Chen, J. Y.; Parkin, G. *J. Am. Chem. Soc.* **1996**, *118*, 7428−7429.

(10) It should be noted that the isolation of the fluoro complex actually requires an additional step, because $Mo(PMe_3)_4H_2F_2$ reacts further with $HF_{(aq)}$ to give a bifluoride derivative. See ref 9.

(11) *trans*-$Mo(PMe_3)_4X_2$ (X = Cl,[a,b] Br,[b,d] I[b,d]) compounds have been previously reported. (a) Carmona, E.; Marin, J. M.; Poveda, M. L.; Atwood, J. L.; Rogers, R. D. *Polyhedron* **1983**, *2*, 185−193. (b) Carmona, E.; Marin, J. M.; Poveda, M. L.; Rogers, R. D.; Atwood, J. L. *J. Am. Chem. Soc.* **1983**, *105*, 3014−3022. (c) Krueger, S. T.; Poli, R.; Rheingold, A. L.; Staley, D. L. *Inorg. Chem.* **1989**, *28*, 4599−4607. (d) Brookhart, M.; Cox, K.; Cloke, F. G. N.; Green, J. C.; Green, M. L. H.; Hare, P. M.; Bashkin, J.; Derome, A. E.; Grebenik, P. D. *J. Chem. Soc., Dalton Trans.* **1985**, 423−433.

(12) While this value for $\Delta S°$ is larger than has been reported for oxidative addition in other systems, and may possibly reflect a systematic error in the data, it should be noted that larger entropy changes have been reported for several other reactions.[a] For example, the dissociation of $\{[Tp^{Pr^iMe}]Co(O_2)\}_2$ is characterized by $\Delta S° = 60(3)$ eu.[b] (a) Minas da Piedade, M.; Martino Simões, J. A. *J. Organomet. Chem.* **1996**, *518*, 167−180. (b) Reinaud, O.; Yap, G. P. A.; Rheingold, A. L.; Theopold, K. H. *Angew. Chem., Int. Ed. Engl.* **1995**, *34*, 2051−2052.

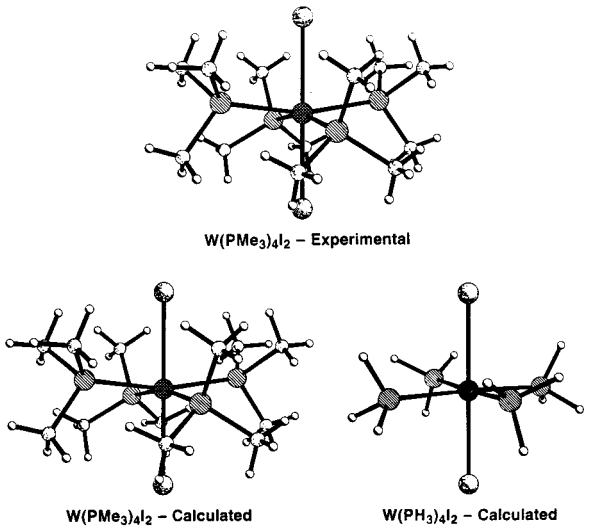

Figure 2. Comparison of the geometry-minimized structures of $W(PMe_3)_4I_2$ and $W(PH_3)_4I_2$ with the experimental structure for the former.

$2D$(W−H),[1b,13] the average W−H bond dissociation energy (BDE) in $W(PMe_3)_4H_2I_2$ has a value of 62.0(6) kcal mol^{-1}.[14] Measurement of this value is of some interest since W−H BDEs have been previously reported for only a few classes of complexes.[15,16]

A knowledge of the factors that influence metal−hydrogen BDEs is central to understanding, and predicting, reaction pathways involving H_2. However, since it was not possible to obtain equilibrium constant data for the other halide systems, we have performed computational studies in an attempt to evaluate the metal and halide dependence of M−H BDEs in the series of molybdenum and tungsten complexes $M(PMe_3)_4H_2X_2$ (M = Mo, W; X = F, Cl, Br, I).

(b) Computational Studies: Geometry-Optimized Molecular Structures and Computed Trends in the Thermodynamics of the Oxidative Addition of H_2. Density functional theory (DFT) calculations were performed on $M(PR_3)_4X_2$[17] and $M(PR_3)_4H_2X_2$ (M = Mo, W; R = H, Me; X = F, Cl, Br, I) complexes using Jaguar (Version 3.5).[18] Geometry-optimized bond length and angle data are listed in the Supporting Information (Tables S2−S5), which also includes experimental values for those trimethylphosphine complexes that have been structurally characterized. A comparison of the experimental and calculated structures is provided in the Experimental Section, but it is important to note here that there is a significant difference in the calculated structures of $M(PH_3)_4X_2$ and $M(PMe_3)_4X_2$. Specifically, the calculated geometries of the PH_3 complexes $M(PH_3)_4X_2$ are approximately octahedral (with all bond angles at M close to 90°), whereas those of $M(PMe_3)_4X_2$ deviate from idealized octahedral coordination due to an alternate up-down "ruffling" of the PMe_3 ligands about the equatorial plane (Figure 2). The latter geometries much more closely resemble the true geometries of $M(PMe_3)_4X_2$, suggesting that the PH_3 ligand is a poor substitute for PMe_3 in theoretical calculations of this system. The discrepancy is undoubtedly a consequence of the lower steric demands of PH_3 *versus* PMe_3.

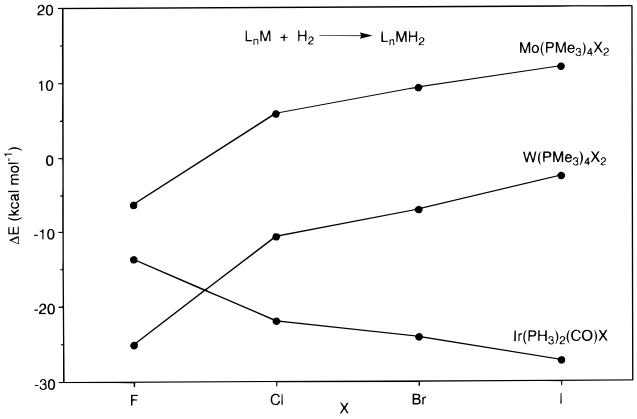

Figure 3. Trends in computed energetics for oxidative addition of H_2 to $M(PMe_3)_4X_2$. For comparison, data for $Ir(PH_3)_2(CO)Cl$, taken from ref 27, are also included.

The energetics of the oxidative addition reactions, as defined by

$$\Delta E = E[M(PR_3)_4H_2X_2] - \{E[M(PR_3)_4X_2] + E[H_2]\}$$

are summarized in Table 3 and Figure 3. The variation in ΔE would be expected to mirror trends in $\Delta H°$, assuming that zero point energy and excitation corrections are similar for each pair of complexes. Support for this assumption is provided by the fact that the difference between $\Delta H°$ and ΔE is very similar for each of the PH_3 derivatives, $W(PH_3)_4F_2$ (+3.1 kcal mol^{-1}), $W(PH_3)_4Cl_2$ (+3.0 kcal mol^{-1}), $W(PH_3)_4Br_2$ (+3.4 kcal mol^{-1}), and $W(PH_3)_4I_2$ (+3.1 kcal mol^{-1}).[19] Furthermore, the correction for addition of H_2 to the PMe_3 complex $W(PMe_3)_4I_2$ is only +0.2 kcal mol^{-1}.

Examination of Table 3 indicates that, even though the overall trend in the energetics of the oxidative addition of H_2 to $M(PH_3)_4X_2$ is similar to that for the $M(PMe_3)_4X_2$ system, the magnitude of the variation in E is substantially greater for the latter. While this difference in thermodynamics may be a result of the different electronic properties of PH_3 and PMe_3, it is more likely a consequence of the different ground-state geometries of $M(PH_3)_4X_2$ and $M(PMe_3)_4X_2$, due to the smaller size of the PH_3 ligand, as described above. In view of this difference in computed structures, it is not surprising that the calculated energetics for oxidative addition to the PH_3 system are different

(13) For rationalization of the use of this expression in determining bond energies, see ref 34 in the following: Hartwig, J. F.; Andersen, R. A.; Bergman, R. G. *Organometallics* **1991**, *10*, 1875−1887.

(14) For dihydrogen, D(H−H) = 104.2 kcal mol^{-1} and D(D−D) = 106.0 kcal mol^{-1}. *CRC Handbook of Chemistry and Physics*, 70th ed.; Weast, R. C., Ed.; CRC Press: Boca Raton, FL, 1989−1990; p F-199.

(15) For examples, see Table S1 in the Supporting Information.

(16) For tabulations of bond energies, see: (a) *Bonding Energetics in Organometallic Compounds*; Marks, T. J. Ed.; ACS Symposium Series 428; American Chemical Society: Washington, DC, 1990. (b) Pearson, R. G. *Chem. Rev.* **1985**, *85*, 41−49. (c) Halpern, J. *Inorg. Chim. Acta* **1985**, *100*, 41−48. (d) Skinner, H. A.; Connor, J. A. *Pure Appl. Chem.* **1985**, *57*, 79−98. (e) Martinho Simões, J. A.; Beauchamp, J. L. *Chem. Rev.* **1990**, *90*, 629−688. (f) Connor, J. A. *Top. Curr. Chem.* **1977**, *71*, 71−110. (g) Wang, K.; Rosini, G. P.; Nolan, S. P.; Goldman, A. S. *J. Am. Chem. Soc.* **1995**, *117*, 5082−5088. (h) Wang, D.; Angelici, R. J. *J. Am. Chem. Soc.* **1996**, *118*, 935−942. (i) Eisenberg, D. C.; Norton, J. R. *Isr. J. Chem.* **1991**, *31*, 55−66. (j) Pilcher, G.; Skinner, H. A. In *The Chemistry of the Metal−Carbon Bond*; Hartley, F. R., Patai, S., Eds.; Wiley: New York, 1982; Vol. 1, Chapter 2, pp 43−90. (k) Labinger, J. A.; Bercaw, J. E. *Organometallics* **1988**, *7*, 926−928. (l) King, W. A.; Di Bella, S.; Gulino, A.; Lanza, G.; Fragala, I. L.; Stern, C. L.; Marks, T. J. *J. Am. Chem. Soc.* **1999**, *121*, 355−366. (m) Hoff, C. D. *Prog. Inorg. Chem.* **1992**, *40*, 503−561. (f) *Energetics of Organometallic Species*; Martinho Simões, J. A., Ed.; Kluwer Academic Publishers: Dordrecht, The Netherlands, 1992.

(17) For theoretical calculations on related chalcogenido complexes, $M(PR_3)_4(E)_2$ (E = O, S, Se, Te), see: (a) Cotton, F. A.; Feng, X. *Inorg. Chem.* **1996**, *35*, 4921−4925. (b) Kim, W.-S.; Kaltsoyannis, N. *Inorg. Chem.* **1998**, *37*, 674−678. (c) Kaltsoyannis, N. *J. Chem. Soc., Dalton Trans.* **1994**, 1391−1400.

(18) Jaguar 3.5, Schrodinger, Inc., Portland, OR, 1998.

(19) The differences between $\Delta H°$ and ΔE are those at 25 °C.

Table 3. Calculated ΔE^a (kcal mol^{-1}) for the Addition of H_2 to $M(PR_3)_4X_2$ (M = Mo, W; X = F, Cl, Br, I; R = H, Me)

	F		Cl		Br		I	
	PH_3	PMe_3	PH_3	PMe_3	PH_3	PMe_3	PH_3	PMe_3
E(Mo)	−2.1	−6.4	1.2	5.8	0.7	9.3	1.7	12.0
E(W)	−19.6	−25.1	−13.3	−10.6	−13.9	−7.1	−12.0	−2.7
E(W) − *E*(Mo)	−17.5	−18.7	−14.7	−16.4	−14.5	−16.4	−13.7	−14.7

[a] $\Delta E = E[M(PR_3)_4H_2X_2] - \{E[M(PR_3)_4X_2] + E[H_2]\}$

Table 4. Estimated M−H BDEs (kcal mol^{-1}) for $M(PMe_3)_4H_2X_2$ (M = Mo, W; X = F, Cl, Br, I), Relative to BDE(W−H) = 62.0 kcal mol^{-1} for $W(PMe_3)_4H_2I_2$

	F	Cl	Br	I
BDE(Mo−H)[a]	63.8	57.7	56.0	54.6
BDE(W−H)[a]	73.2	66.0	64.2	62.0
BDE(W−H) − BDE(Mo−H)	9.4	8.2	8.2	7.4

[a] $BDE(M_X{-}H) = 0.5[E_{WI} - E_{MX} + 124]$.

from those of the PMe_3 system, with the latter presumably providing a much better estimate of the true values. Jacobsen and Berke have also recently noted that it is important to use the real ligand, PMe_3, rather than PH_3 in calculations to assess relative energies of isomers of $[Fe(PMe_3)_4H_3]^+$.[20]

Figure 3 indicates that the exoergicity of the oxidative addition of H_2 to $M(PMe_3)_4X_2$ strongly increases in the sequences (i) Mo < W and (ii) I < Br < Cl < F. Since the thermodynamic differences are directly related to the differences in M−H bond energies as defined above, the M−H bond energies may be estimated by appropriate scaling with respect to the experimentally determined value of 62.0(6) kcal mol^{-1} for the average W−H bond energy of $W(PMe_3)_4H_2I_2$ (Table 4). Inspection of Table 4 indicates that the W−H bond energies are ca. 7−10 kcal mol^{-1} greater than the corresponding Mo−H energies, in line with other reports of bond energies for third- and second-row transition metals.[15,21,22] For example, the W−H bond in Cp_2WH_2 (74.3 kcal mol^{-1}) is 12.9 kcal mol^{-1} stronger than the Mo−H bond in Cp_2MoH_2 (61.4 kcal mol^{-1}).[23] Such increases in M−H bond energies from the first to third series are typically attributed to more favorable sd hybridization, coupled with a greater radial extent of the hybrid orbital for the heavier elements, which results in increased overlap with the hydrogen 1s orbital.[24]

Of most interest, the influence of the halide on the thermodynamics of the oxidative addition of H_2 is completely counter to that reported for oxidative addition of H_2 to Vaska-type complexes, *trans*-$Ir(PR_3)_2(CO)X$. Thus, early experimental studies by Vaska on *trans*-$Ir(PPh_3)_2(CO)X$,[25,26] and a computational study by Goldman and Krogh-Jespersen on *trans*-$Ir(PH_3)_2(CO)X$,[27] indicate that oxidative addition of H_2 to iridium in these complexes becomes progressively more exothermic upon passing from the fluoro to iodo derivatives (Table 5 and Figure 3). To understand the origin of the striking difference between these two systems, it is essential to understand how, and why, various substituents influence the susceptibility of a metal center towards oxidative addition. In this regard, it is commonly assumed that the ability of a metal center to undergo an oxidative addition reaction is directly related to its electron richness, i.e., "factors that tend to increase the electron density on the metal make for an increase in oxidizability".[28−30] For example, the equilibrium constants for the oxidative addition of H_2 to *trans*-$Ir(PR_3)_2(CO)Cl$ increase as the σ-donor PR_3 ligands become more basic.[31] Likewise, the equilibrium constants for oxidative addition of $PhCO_2H$ to *trans*-$Ir(PR_3)_2(CO)X$ (X = Cl, Br, I), giving *trans*-$Ir(PR_3)_2(CO)X(O_2CPh)H$, also increase with the basicity of PR_3 in the sequence PPh_3 < $PMePh_2$ < PMe_2Ph < PMe_3.[32]

While the observed halide dependence for oxidative addition of H_2 to $Ir(PR_3)_2(CO)X$ is in accord with that expected on the basis of the variation of the halogen electronegativity,[33] it is important to note that this order is counter to that which would be predicted by the *overall* electron-donating ability of the halogens. Specifically, the overall electron-donating ability of a halogen toward a transition metal decreases in the sequence F > Cl > Br > I, a consequence of the trend being dictated by the stronger π-donation of the lighter halogens.[34,35] Thus, although the electron richness of the iridium centers, as judged by the ν(CO) stretching frequencies of *trans*-$Ir(PPh_3)_2(CO)X$, *decreases* in the order F > Cl > Br > I,[36,37] the tendency to oxidatively add H_2 *increases* in the order F < Cl < Br < I

(20) Jacobsen, H.; Berke, H. *Chem. Eur. J.* **1997**, *3*, 881−886.

(21) Kinetic barriers to reductive elimination of H_2 from a metal center follow a similar trend, with the barriers being greater for the heavier metal. See, for example: Halpern, J.; Cai, L.; Desrosiers, P. J.; Lin, Z. *J. Chem. Soc., Dalton Trans.* **1991**, 717−723.

(22) M−C bond energies also increase upon descending a transition metal group. See, for example: Mancuso, C.; Halpern, J. *J. Organomet. Chem.* **1992**, *428*, C8−C11.

(23) Dias, A. R.; Martinho Simões, J. A. *Polyhedron* **1988**, *7*, 1531−1544.

(24) (a) Ohanessian, G.; Goddard, W. A., III. *Acc. Chem. Res.* **1990**, *23*, 386−392. (b) Landis, C. R.; Firman, T. K.; Root, D. M.; Cleveland, T. *J. Am. Chem. Soc.* **1998**, *120*, 1842−1854.

(25) Vaska, L.; Werneke, M. F. *Ann. N.Y. Acad. Sci.* **1971**, *172*, 546−562.

(26) It should be noted that the Vaska system had also been studied by Strohmeier, who obtained results that are not in accord with Vaska's. See: Strohmeier, W.; Müller, F. J. *Z. Naturforsch.* **1969**, *24b*, 931−932.

(27) (a) Abu-Hasanayn, F.; Krogh-Jespersen, K.; Goldman, A. S. *Inorg. Chem.* **1993**, *32*, 495−496. (b) Abu-Hasanayn, F.; Goldman, A. S.; Krogh-Jespersen, K. *Inorg. Chem.* **1994**, *22*, 5122−5130.

(28) Cotton, F. A.; Wilkinson, G. *Advanced Inorganic Chemistry*, 5th ed.; Wiley: New York, 1988; p 1191.

(29) (a) Collman, J. P. *Acc. Chem. Res.* **1968**, *1*, 136−141. (b) Collman, J. P.; Roper, W. R. *Adv. Organomet. Chem.* **1968**, *7*, 53−94.

(30) Crabtree has suggested that some oxidative addition reactions of H_2, in which the addition is inhibited in the presence of certain donor ligands such as halide, should be regarded as "reductive" in nature.[a] With respect to such a viewpoint, it is pertinent to quote from the work of Saillard and Hoffmann: "Formalisms are convenient fictions which contain a piece of the truth—and it is so sad that people spend a lot of time arguing about the deductions they draw, often ingeniously and artfully, from formalisms, without worrying about their underlying assumptions. The 'complex' or dative bonding picture which led to 'oxidation at metal' of course is an exaggeration. The M−H σ bonds are in good part covalent. To the extent that they are so, the real *d* electron population at the metal moves back from d^{n-2} toward d^n. To the extent that it probably never quite gets back to d^n it is still informative to call this an oxidative addition." [b] (a) Crabtree, R. H.; Quirk, J. M. *J. Organomet. Chem.* **1980**, *199*, 99−106. (b) Saillard, J.-Y.; Hoffmann, R. *J. Am. Chem. Soc.* **1984**, *106*, 2006−2026.

(31) Specifically, equilibrium constants (at 30 °C) for addition of H_2 to *trans*-$Ir(PR_3)_2(CO)Cl$ are 3.2×10^4 M^{-1} (R = C_6H_5), 4.4×10^4 M^{-1} (R = C_6H_4Me), and 5.2×10^4 M^{-1} (R = C_6H_4OMe). Furthermore, the complex with R = C_6F_5 was unreactive toward H_2. See ref 25.

(32) (a) Deeming, A. J.; Shaw, B. L. *J. Chem. Soc. (A)* **1969**, 1802−1804. (b) van Doorn, J. A.; Masters, C. van der Woude, C. *J. Chem. Soc., Dalton Trans.* **1978**, 1213−1220.

(33) Furthermore, oxidative addition of $PhCO_2H$ to *trans*-$Ir(PR_3)_2(CO)X$ (X = Cl, Br, I) becomes more favored in the sequence Cl < Br < I. See ref 32.

(34) (a) Caulton, K. G. *New J. Chem.* **1994**, *18*, 25−41. (b) Caulton, K. G. *Chemtracts—Inorg. Chem.* **1993**, *5*, 170−172.

Table 5. Halogen Dependence of the Thermodynamics for Addition of H_2 to a Metal Center

reactant	product	$\Delta H°$ (kcal mol^{-1})	$\Delta S°$ (eu)	refs
$Ir(PPh_3)_2(CO)X$	$Ir(PPh_3)_2(CO)H_2X$			25, 27b[b]
X = F		> −10 [−13.6][a]		
X = Cl		−14.4(8) [−22.0][a]	−26(2.4)	
X = Br		−17.0(6) [−24.1][a]	−31(2.0)	
X = I		−18.8(8) [−27.3][a]	−27(3.2)	
$Ir(PBu^t_2Ph)_2H_2X$	$Ir(PBu^t_2Ph)_2H_2(\eta^2\text{-}H_2)X$			41b
X = Cl		−6.8(2)	−19.2(7)	
X = Br		−7.9(9)	−19.7(3.2)	
X = I		−9.3(2)	−22.7(1.8)	
$Ir(PPr^i_3)_2H_2X$	$Ir(PPr^i_3)_2H_2(\eta^2\text{-}H_2)X$			56[c]
X = Cl		−12.3(3)	−37(3)	
X = Br		−12.0(2)	−33(3)	
X = I		−10.2(4)	−23(3)	

[a] Values in brackets are computed ΔE(MP4) values for addition of H_2 to $Ir(PH_3)_2(CO)X$. [b] Reference 62, p 187. [c] Equilibrium data listed are for *n*-hexane solution. Values for toluene and methylcyclohexane were also reported.

(Table 5). Although this observation seems paradoxical, calculations by Krogh-Jespersen and Goldman on addition of H_2 to *trans*-$Ir(PH_3)_2(CO)X$ (X = Cl, Br, I, NH_2, PH_2) indicate that the presence of occupied π-orbitals on X strongly disfavors oxidative addition.[38] Specifically, π-interactions have the ability to stabilize the "16-electron" *trans*-$Ir(PH_3)_2(CO)X$ reactant[39] but destabilize the 18-electron dihydride product *trans*-$Ir(PPh_3)_2(CO)(X)H_2$ via "$d_\pi - p_\pi$ filled−filled repulsions".[34a,40] Such interactions would be greatest for the fluoride derivative, which therefore exhibits the least tendency to oxidatively add H_2.[41] An important issue, therefore, is concerned with why the "16-electron" molybdenum and tungsten complexes $M(PMe_3)_4X_2$ do not behave analogously to the Vaska system and instead exhibit a completely opposite trend with respect to oxidative addition.

Since oxidative addition of H_2 involves an increase in coordination number, steric interactions would be expected to be least favorable for the largest halide derivative. The fact that the largest halide derivative, *trans*-$Ir(PPh_3)_2(CO)I$, oxidatively adds H_2 most exothermically indicates that electronic factors (as described above) must dominate over the steric factors and be responsible for the observed trend in the Vaska system. For the molybdenum and tungsten systems, however, steric effects may be expected to be more influential in determining the thermodynamics since the product of oxidative addition is eight-coordinate, rather than six-coordinate as in $Ir(PPh_3)_2(CO)(X)H_2$. Thus, the observed halide dependence for oxidative addition of H_2 to $M(PMe_3)_4X_2$ is consistent with the thermodynamics being dictated by steric effects. However, there is also an electronic rationalization for the observed trend, which is concerned with the fact that the four π-symmetry orbitals of the two *trans*-X atoms in $M(PMe_3)_4X_2$ (with D_{2d} symmetry) belong to two sets of *E* symmetry orbitals, one pair of which interacts with the d_{xz} and d_{yz} orbitals (Figure 4). Since the antibonding component of this interaction (the metal-based 3e* HOMO) is occupied by two electrons, the energy of the system is raised as the strength of the π-donor interaction increases

(35) For example: (i) the enthalpy of protonation of a variety of $[Cp^R]M(PR_3)X$ (M = Ru, Os) derivatives indicates that the basicity of the metal center increases in the sequence I < Br < Cl.[a,b] (ii) Spectroscopic and electrochemical studies on *trans*-$M(PPh_3)_2(CO)X$ (M = Rh, Ir),[c] $CpRe(NO)(PPh_3)X$,[d] and $CpRe(NO)(CO)X$[d] indicate that the fluoro complexes have the most electron-rich metal centers. Curiously, however, the opposite trend is observed for $[(tacn)Re(NO)(CO)X]^+$, for which ν(CO) and ν(NO) stretching frequencies decrease in the order F > Cl > Br > I.[e] (iii) $^1J_{Si-H}$ coupling constants and ν_{Si-H} stretching frequencies for $Cp_2Zr(NBu^t\text{-}SiMe_2H)X$, which exhibit three-center, two-electron Zr−H−Si interactions, increase in the sequence H < I < Br < Cl < F, indicating that the zirconium center of the fluoro complex exhibits the lowest electrophilicity.[f] (iv) ESR and electronic spectroscopic studies on Cp^*_2TiX complexes indicate that the π-interactions increase in the sequence I < Br < Cl < F.[g] (v) Electrochemical studies on Cp_2MX_2 (M = Nb, Ta)[h] and $Cp_2W(R)X$[i] indicate that the ease of oxidation increases in the sequence I < Br < Cl. (a) Rottink, M. K.; Angelici, R. J. *J. Am. Chem. Soc.* **1993**, *115*, 7267−7274. (b) Rottink, M. K.; Angelici, R. J. *J. Am. Chem. Soc.* **1992**, *114*, 8296−8298. (c) Doherty, N. M.; Hoffman, N. W. *Chem. Rev.* **1991**, *91*, 553−573. (d) Agbossou, S. K.; Roger, C.; Igau, A.; Gladysz, J. A. *Inorg. Chem.* **1992**, *31*, 419−424. (e) Pomp, C.; Wieghardt, K. *Inorg. Chem.* **1988**, *27*, 3796−3804. (f) Procopio, L. J.; Carroll, P. J.; Berry, D. H. *J. Am. Chem. Soc.* **1994**, *116*, 177−185. (g) Lukens, W. W., Jr.; Smith, M. R., III; Andersen, R. A. *J. Am. Chem. Soc.* **1996**, *118*, 1719−1728. (h) Hunter, J. A.; Lindsell, W. E. McCullough, K. J.; Parr, R. A.; Scholes, M. L. *J. Chem. Soc., Dalton Trans.* **1990**, 2145−2153. (i) Asaro, M. F.; Cooper, S. R.; Cooper, N. J. *J. Am. Chem. Soc.* **1986**, *108*, 5187− 5193.

(36) ν(CO)/cm^{-1} for *trans*-$Ir(PPh_3)_2(CO)X$: 1957 (F), 1965 (Cl), 1966 (Br), and 1967 (I). See: Vaska, L.; Peone, J., Jr. *J. Chem. Soc., Chem. Commun.* **1971**, 418−419.

(37) Goldman and Krogh-Jespersen have offered another suggestion to account for the observed variation of ν(CO) stretching frequencies in the Vaska system. Specifically, they have attributed the observed ν(CO) trend to the greater electrostatic field strength of the lighter halides, which raises the energy of the Ir d orbitals and, as a consequence, promotes π-back-bonding to CO. See ref 27b.

(38) Whereas occupied π-orbitals on the halide substituents strongly disfavor oxidative addition to $Ir(PR_3)_2(CO)X$, Goldman and Krogh-Jespersen have calculated that substituents with π-acceptor orbitals, such as BH_2, would promote oxidative addition by stabilizing the 18-electron product. See ref 27b.

(39) The precise nature of π-donation in square planar d^8 complexes deserves some comment since the only unoccupied d orbital, i.e. the $d_{x^2-y^2}$, lies along the ligand axes and so is incapable of π-overlap with halogen p orbitals. However, in the presence of a *trans* π-acceptor ligand such as CO, interactions with d_{yz} and d_{xz} (with the halogen located on the *z* axis) become possible via a "push/pull" mechanism.[a] It is also possible that π-interactions may occur with metal p orbitals. For example, calculations suggest that the PH_2 ligand in $(H_3P)_3RhPH_2$ is coplanar with the RhP_3 group due to favorable P(p)−Rh(p) π-interactions.[b] In contrast, however, calculations suggest that there are no substantial π-interactions involving a Pt(p) orbital in $(H_3P)_2Pt(H)(NH_2)$.[c] (a) Reference 34a. (b) Dahlenburg, L.; Höck, N.; Berke, H. *Chem. Ber.* **1988**, *121*, 2083−2093. (c) Cowan, R. L.; Trogler, W. C. *J. Am. Chem. Soc.* **1989**, *111*, 4750−4761.

(40) The overlap of filled orbitals results in a repulsive interaction because the antibonding orbital is destabilized to a greater extent than the bonding orbital is stabilized. For example, the overlap of two identical orbitals results in a bonding orbital that is stabilized by an energy $\Delta/(1 + S)$, while the antibonding combination is destabilized by $\Delta/(1 - S)$, where Δ is the interaction energy and *S* is the overlap integral. See: Albright, T. A.; Burdett, J. K.; Whangbo, M.-H. *Orbital Interactions in Chemistry*; Wiley: New York, 1985.

(41) Goldman and Krogh-Jespersen have also used ab initio calculations to study the transition-state properties for addition of H_2 to Vaska-type complexes, *trans*-$Ir(L)_2(CO)X$ (L = PH_3 and X = F, Cl, Br, I, CN, H), and have concluded that strong π-donation increases the barrier to oxidative addition.[a] Likewise, Caulton has reported that the activation barriers for coordinating H_2 to $Ir(PBu^t_2Me)_2H_2X$ increase in the order I < Br < Cl, with the better π-donor inhibiting binding.[b] Conversely, the activation barrier for elimination of H_2 follows the opposite trend, with Cl having the lower barrier since π-donation promotes elimination. (a) Abu-Hasanayn, F.; Goldman, A. S.; Krogh-Jespersen, K. *J. Phys. Chem.* **1993**, *97*, 5890−5896. (b) Hauger, B. E.; Gusev, D.; Caulton, K. G. *J. Am. Chem. Soc.* **1994**, *116*, 208−214.

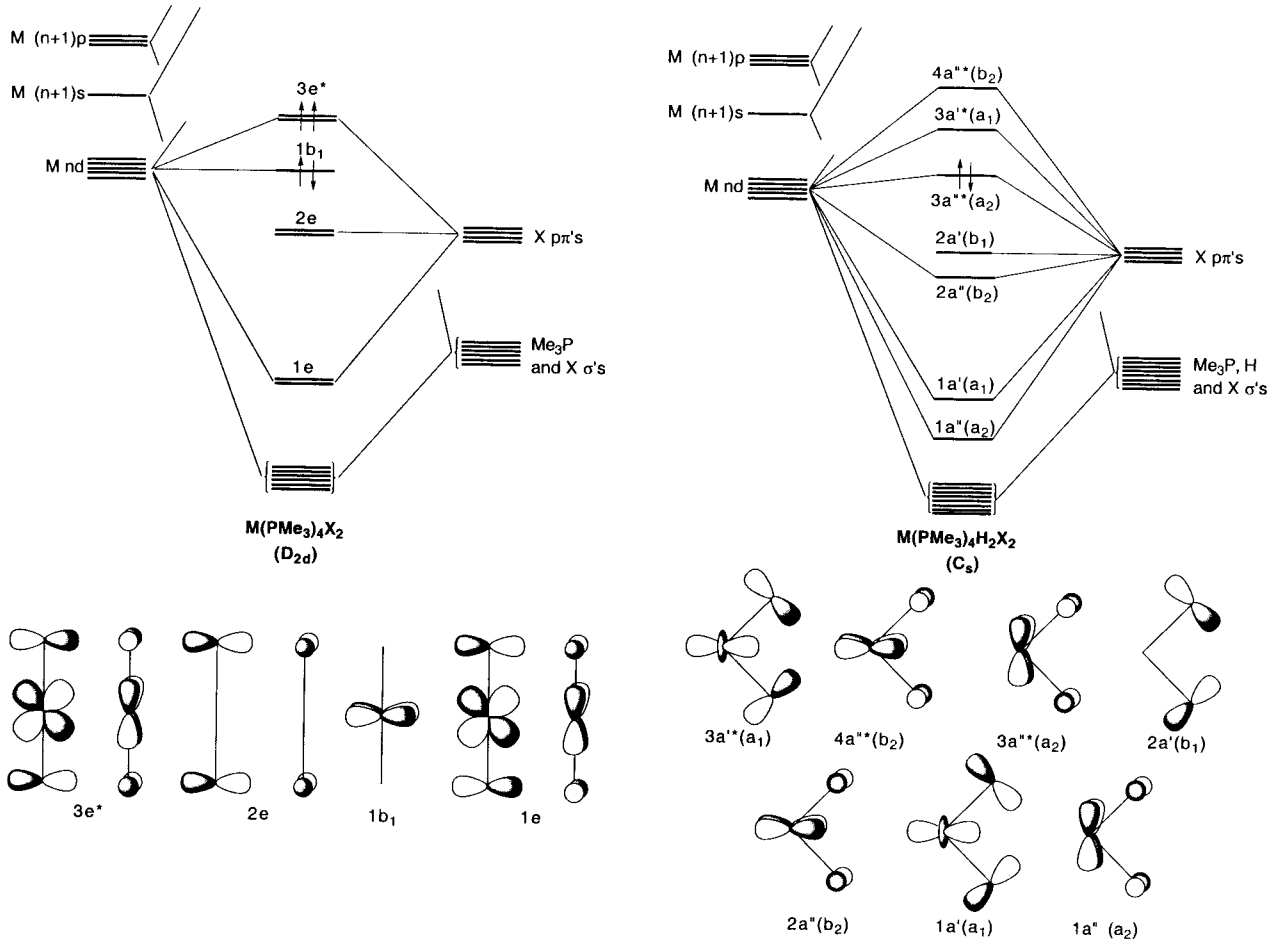

Figure 4. Qualitative MO diagrams for $M(PMe_3)_4X_2$ (D_{2d}) and $M(PMe_3)_4H_2X_2$ (C_s). The symmetry labels in parentheses for $M(PMe_3)_4H_2X_2$ are those for idealized C_{2v} symmetry.

(Figure 4).[42] Consequently, ground-state destabilization of $M(PMe_3)_4X_2$ electronically promotes oxidative addition for the better π-donor. This marked instability of the fluoride complexes $M(PMe_3)_4F_2$ with respect to $M(PMe_3)_4H_2F_2$ has a close parallel with the observation that terminal oxo complexes of the late transition metals are very rare.[43] Specifically, Mayer has rationalized the paucity of such complexes to be a result of repulsive π-interactions between oxygen "lone pairs" and filled d orbitals.[44]

In an attempt to differentiate the electronic and steric components, it is instructive to consider the oxidative addition as proceeding via a *hypothetical* sequence involving first a structural reorganization of *trans*-$M(PMe_3)_4X_2$ to a *cis* geometry (with the PMe_3 and X ligands located in the same positions that they occupy in eight-coordinate $M(PMe_3)_4H_2X_2$), followed by addition of H_2. The relative energies for these processes are summarized in Figure 5 for the tungsten system, with the energy of the hypothetical *cis*-$W(PMe_3)_4X_2$ entities arbitrarily fixed at a common value for comparison purposes.

To a *first approximation*, steric factors would be expected to play a more important role in the structural reorganization step

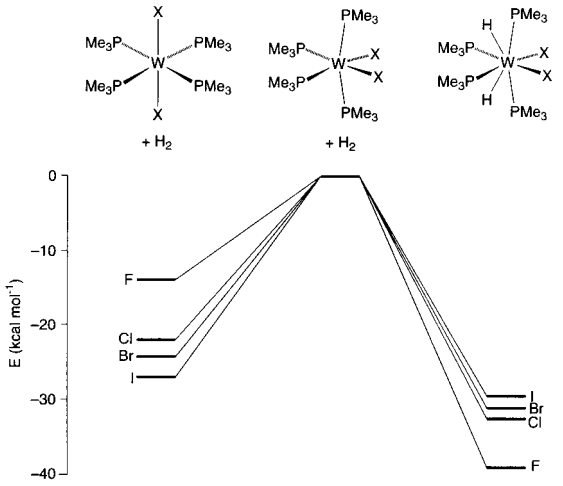

Figure 5. Structural reorganization and intrinsic bond energy components for oxidative addition of H_2. The energies of *cis*-$W(PMe_3)_4X_2$ are arbitrarily fixed at a common value.

than in the oxidative addition step. This statement is not intended to imply that electronic factors do not play a role in the structural reorganization step. Indeed, π-interactions would be expected to destabilize a *cis* geometry for a d^4 octahedral complex of the type ML_4X_2, by virtue of the fact that a formally nonbonding occupied orbital (b_{2g}) in the *trans* arrangement becomes antibonding in the *cis* structure, as illustrated schematically in Figure 6. As such, the strongest π-donor ligand, fluorine, would be expected to *electronically* disfavor structural rearrangements

(42) Calculations on the series of d^0 complexes, Cp_2TiX_2 (X = F, Cl, Br, I), also indicate that the orbital energies vary in a similar way to those in $Mo(PMe_3)_4X_2$. See: Bruce, M. R. M.; Kenter, A.; Tyler, D. R. *J. Am. Chem. Soc.* **1984**, *106*, 639−644.

(43) See, for example: (a) Nugent, W. A.; Mayer, J. M. *Metal−Ligand Multiple Bonds*; Wiley-Interscience: New York, 1988. (b) Trnka, T. M.; Parkin, G. *Polyhedron* **1997**, *16*, 1031−1045. (c) Parkin, G. *Prog. Inorg. Chem.* **1998**, *47*, 1−165.

(44) Mayer, J. M. *Comments Inorg. Chem.* **1988**, *8*, 125−135.

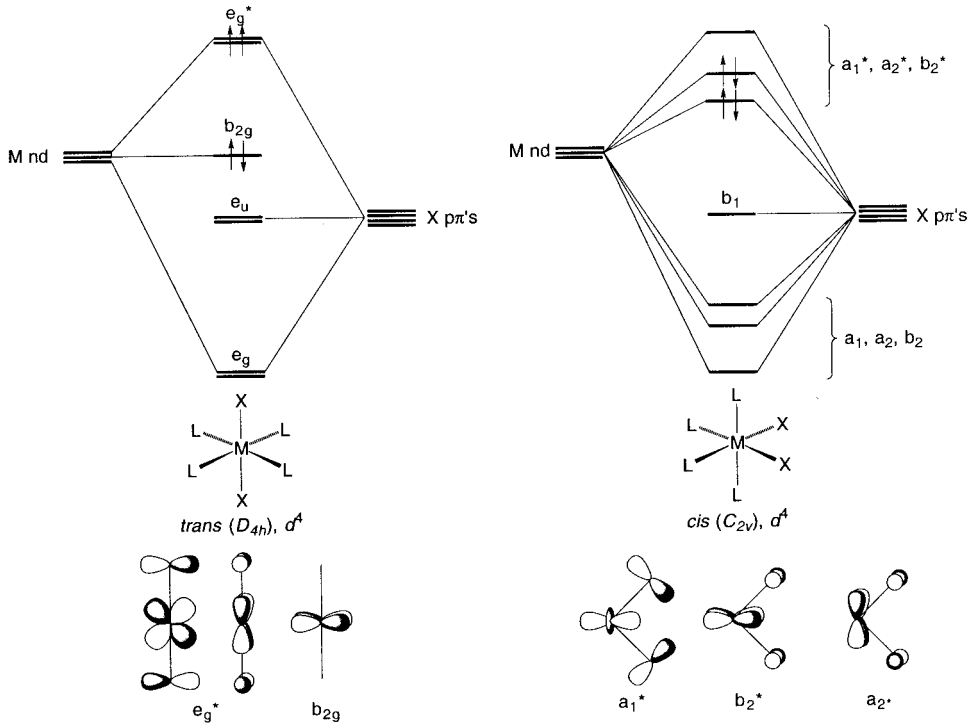

Figure 6. Qualitative MO diagrams for *cis* and *trans* ML_4X_2.

from a *trans* structure.[45] Since electronic factors disfavor a *trans*-to-*cis* rearrangement most for the fluoride derivative, the result that the first step of the hypothetical transformation is least endothermic for the fluoride derivative strongly suggests that the structural reorganization is dominated by steric factors.

The second step of the hypothetical transformation is also most exothermic for the fluoride derivative; this step corresponds to the *intrinsic* W−H bond energy of $W(PMe_3)_4H_2X_2$, i.e., that without allowing for molecular relaxation. Since the hydride ligand is small, the energetics of the latter step would be anticipated to be more a reflection of electronic factors, and the trend is consistent with the notion that π-donation within $W(PMe_3)_4X_2$ destabilizes the system with respect to oxidative addition by population of antibonding levels. It is therefore suggested that steric and electronic factors may serve to reinforce each other in promoting oxidative addition most for the fluoride derivative $W(PMe_3)_4F_2$.

Support for the notion that electronic factors contribute to making oxidative addition most favored for the fluoride derivatives is provided by analyzing the variation in energies of the highest occupied molecular orbitals of $M(PMe_3)_4X_2$ and $M(PMe_3)_4H_2X_2$. Plots of the energies of these orbitals obtained from the DFT calculations are shown in Figure 7. The HOMOs for each of the $M(PMe_3)_4X_2$ species are a pair of half-occupied degenerate 3e* orbitals, corresponding to the metal-based d_{xz} and d_{yz} orbitals that are antibonding by virtue of their π-interaction with the halogen *p* orbitals. Notably, the energy of the HOMO increases dramatically from the iodo to fluoro derivatives (Figure 7), due to enhanced π-interactions, so that its occupation strongly destabilizes $M(PMe_3)_4X_2$ with respect to $M(PMe_3)_4H_2X_2$. It is important to point out that the 3a″* HOMO of $M(PMe_3)_4H_2X_2$, which is principally the metal d_{yz} orbital,[46] is less sensitive to the nature of the halogen than is the 3e* HOMO in $M(PMe_3)_4X_2$, so that its occupation does not dictate the thermodynamics of the interconversion (Figure 7). In

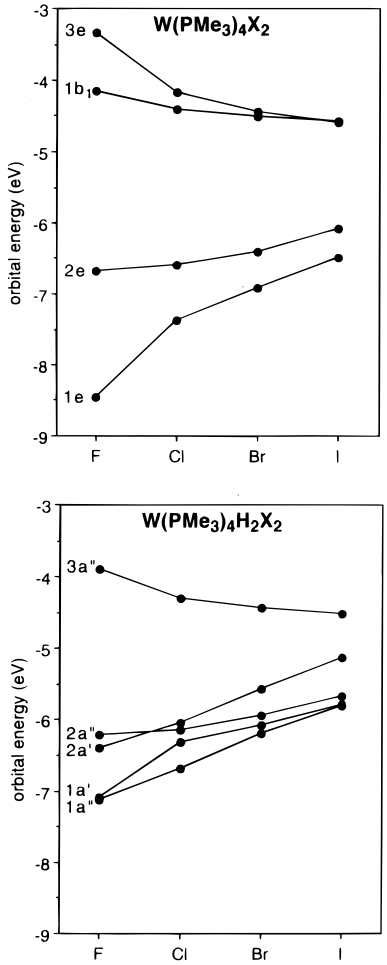

Figure 7. Variation of the highest occupied orbitals in $W(PMe_3)_4X_2$ and $W(PMe_3)_4H_2X_2$. The Mo system is similar.

(45) Arguments of this type have been used previously to rationalize the *trans* (as opposed to *cis*) arrangement of octahedral d^2 dioxo complexes, $[ML_4(O)_2]$. See, for example, ref 43a.

(46) For $M(PH_3)_4H_2X_2$ (C_{2v}), the HOMO is of a_2 symmetry and is principally the d_{xy} orbital.

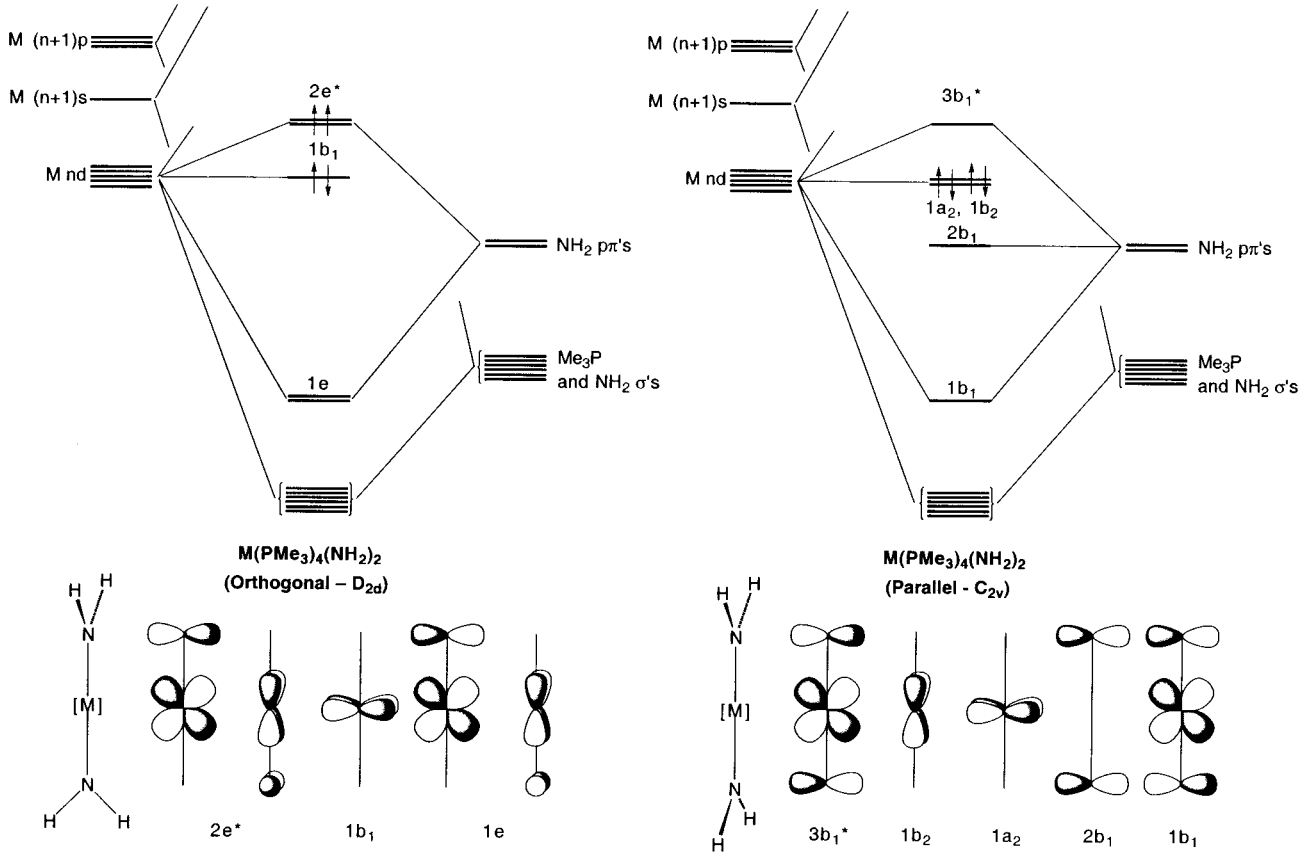

Figure 8. Qualitative MO diagrams for $M(PMe_3)_4(NH_2)_2$ with parallel and orthogonal orientations of the NH_2 ligands.

essence, "filled−filled" repulsions are more dominant in $M(PMe_3)_4X_2$ than in $M(PMe_3)_4H_2X_2$,[47] with the result that oxidative addition is most favored for the fluoride derivatives. It is noteworthy that, although the average M−H BDEs for $M(PMe_3)_4H_2X_2$ increase in the sequence I < Br < Cl < F, the experimental ν_{W-H} stretching frequencies for $W(PMe_3)_4H_2X_2$ exhibit the opposite trend: F (1835 and 1900 cm^{-1}), Cl (1933 cm^{-1}), Br (1934 cm^{-1}), I (1961 cm^{-1}).[48,49] Thus, counterintuitively, M−H stretching frequencies in a related series of complexes are not necessarily good indicators of trends in bond strengths.[50] In this regard, it should be noted that stronger bonds do not always correlate with shorter bonds of the same type.[51]

A further illustration of the way in which π-donation influences oxidative addition of H_2 is provided by calculations on two isomers of *trans*-$M(PMe_3)_4(NH_2)_2$, which differ according to whether the NH_2 groups are parallel (C_{2v} symmetry) or orthogonal (D_{2d} symmetry) to each other. Unlike halide substituents that have two π-donor orbitals, the NH_2 group has only a single π-donor function. Furthermore, depending upon the relative orientation of the two NH_2 groups, the π-interactions within *trans*-$M(PMe_3)_4(NH_2)_2$ could be with either a single d orbital or two different d orbitals, as illustrated in Figure 8. The former possibility is in marked contrast to the halide complexes $M(PMe_3)_4X_2$, for which π-interactions must occur in a pairwise manner with two d orbitals.[52] Significantly, oxidative addition of H_2 to the orthogonal (D_{2d}) isomer of the tungsten complex $W(PMe_3)_4(NH_2)_2$ is calculated to be substantially more exothermic by 13.9 kcal mol^{-1} than that for the parallel (C_{2v}) arrangement.[53] Since the product of oxidative addition, i.e., $W(PMe_3)_4H_2(NH_2)_2$, is the same for both reactions, the difference in exothermicity directly reflects the relative stabilities of the two isomers of $W(PMe_3)_4(NH_2)_2$. Examination of Figure 8 indicates that the parallel (C_{2v}) isomer is the more stable because the p orbitals of both NH_2 groups interact with the same metal d orbital, such that the "d^4" electrons occupy two formally nonbonding d orbitals. In contrast, the p orbitals

(47) Presumably this is a consequence of increased π-overlap for the *trans* MX_2 fragment as compared to that for a bent geometry (see Figures 4 and 5).

(48) (a) Reference 4. (b) Green, M. L. H.; Parkin, G.; Chen, M.; Prout, K. *J. Chem. Soc., Dalton Trans.* **1986**, 2227−2236.

(49) Values in toluene solution are F, 1839 and 1882 cm^{-1}; Cl, 1917 cm^{-1}; Br, 1933 cm^{-1}; and I, 1959 cm^{-1}. Computational studies on $W(PH_3)_4H_2X_2$ reproduce this trend. Thus, calculated ν_{W-H} stretching frequencies (A_1 and B_2 symmetry) for $W(PH_3)_4H_2X_2$ are F, 1844 and 1835 cm^{-1}; Cl, 1893 and 1883 cm^{-1}; Br, 1897 and 1892 cm^{-1}; and I 1900 and 1892 cm^{-1}.

(50) The experimental and calculated W−H stretching frequencies do, however, qualitatively correlate with the calculated W−H bond lengths listed in Table S5, in accord with Badger's rule, $k = [a_{ij}(r_e - d_j)]^{-3}$, where k is the force constant, r_e is the equilibrium bond length, and a_{ij} and d_{ij} are constants.[a−d] Exceptions to Badger's rule are, nevertheless, known.[e] (a) Badger, R. M. *J. Chem. Phys.* **1934**, *2*, 128−131. (b) Badger, R. M. *J. Chem. Phys.* **1935**, *3*, 710−714. (c) Herschbach, D. R.; Laurie, V. W. *J. Chem. Phys.* **1961**, *35*, 458−463. (d) Pauling, L. *The Nature of The Chemical Bond*, 3rd ed.; Cornell University Press: Ithaca, NY, 1960; p 231. (e) Christen, D.; Gupta, O. D.; Kadel, J.; Kirchmeier, R. L.; Mack, H. G.; Oberhammer, H.; Shreeve, J. M. *J. Am. Chem. Soc.* **1991**, *113*, 9131−9135.

(51) See, for example: (a) Ernst, R. D.; Freeman, J. W.; Stahl, L.; Wilson, D. R.; Arif, A. M.; Nuber, B.; Ziegler, M. L. *J. Am. Chem. Soc.* **1995**, *117*, 5075−5081. (b) Tudela, D. *J. Chem. Educ.* **1996**, *73*, A297. (c) Boyd, S. L.; Boyd, R. J. *J. Am. Chem. Soc.* **1997**, *119*, 4214−4219. (d) Mayer, P. M.; Glukhovtsev, M. N.; Gauld, J. W.; Radom, L. *J. Am. Chem. Soc.* **1997**, *119*, 12889−12895. (e) Bowmaker, G. A.; Schmidbaur, H.; Krüger, S.; Rösch, N. *Inorg. Chem.* **1997**, *36*, 1754−1757. (f) McKean, D. C.; Torto, I.; Morrison, A. R. *J. Phys. Chem.* **1982**, *86*, 307−309. (g) Vollhardt, K. P. C.; Cammack, J. K.; Matzger, A. J.; Bauer, A.; Capps, K. B.; Hoff, C. D. *Inorg. Chem.* **1999**, *38*, 2624−2631.

(52) For an example of the influence of selective π-interactions stabilizing unusual oxo complexes, see: Bursten, B. E.; Cayton, R. H. *Organometallics* **1987**, *6*, 2004−2005.

(53) ΔE for addition to the parallel (C_{2v}) isomer is −3.1 kcal mol^{-1}, while that for addition to the orthogonal (D_{2d}) isomer is −17.0 kcal mol^{-1}.

of the NH_2 groups of the orthogonal (D_{2d}) isomer interact with two different metal d orbitals, so that only one d orbital remains formally nonbonding. As a consequence, a pair of electrons is forced to occupy an antibonding orbital (i.e., a "filled−filled" repulsion), which destabilizes the structure relative to that of the parallel (C_{2v}) isomer. The latter situation is closely analogous to that in the halide $M(PMe_3)_4X_2$ derivatives. Therefore, consideration of the stabilities of the two isomers of $W(PMe_3)_4(NH_2)_2$, in which differences in steric interactions are likely to be negligible, emphasizes the important role that π-interactions have in influencing the energetics of oxidative addition of H_2 to $M(PMe_3)_4X_2$ complexes.

A principal distinction between the $M(PMe_3)_4X_2$ and Vaska systems is that, because of the molecular symmetry, π-donation within $M(PMe_3)_4X_2$ must occur in a *pairwise* manner; i.e., it is not possible to partake in a selective π-interaction with a *single* metal orbital. In contrast, the molecular symmetry of *trans*-$Ir(PPh_3)_2(CO)X$ is such that the two p orbitals on X are not degenerate, so that it is possible for a selective π-interaction between a p orbital on X and a single metal orbital to occur without requiring excessive "filled−filled" repulsions with the other nonbonding X p orbital. An alternative, simplified, view of the situation is that π-donation within 16-electron *trans*-$Ir(PPh_3)_2(CO)X$ may stabilize the molecule by transforming it into an "18-electron" complex,[39] whereas π-donation within 16-electron $M(PMe_3)_4X_2$ must *destabilize* the molecule by transforming it into a "20-electron" complex. However, it is essential to also consider the factors influencing the stabilities of the products of oxidative addition in order to rationalize fully the halide dependence. Having 18-electron configurations, both $M(PMe_3)_4H_2X_2$ and *trans*-$Ir(PPh_3)_2(CO)(H)_2X$ will exhibit "filled−filled" repulsions, but such interactions are likely to be exacerbated for the d^6 Vaska system since the octahedral geometry is ideally suited for π-interactions with *both* halogen p orbitals. In contrast, as a result of the less regular symmetry of the eight-coordinate complexes $M(PMe_3)_4H_2X_2$, not all of the halogen p orbitals interact efficiently with the metal d orbitals; thus, unfavorable "side-on" overlap, of the type illustrated by the $3a''(a_2)$ HOMO in Figure 4, results in less destabilization. Consequently, "filled−filled" repulsions most likely destabilize *trans*-$Ir(PPh_3)_2(CO)(H)_2X$ to a greater extent than those for $M(PMe_3)_4H_2X_2$ with respect to reductive elimination of H_2.

The electronic components of the oxidative addition of H_2 to $M(PMe_3)_4X_2$ and *trans*-$Ir(PPh_3)_2(CO)X$ may, therefore, be rationalized according to the influence of "filled−filled" repulsions on the reactants and products. In essence, π-antibonding interactions are proposed to be (i) greater in $M(PMe_3)_4X_2$ than those in $Ir(PPh_3)_2(CO)X$ and (ii) greater in $Ir(PPh_3)_2(CO)(H)_2X$ than those in $M(PMe_3)_4H_2X_2$. As a result, π-donor ligands exert an opposite influence on the oxidative addition of H_2 to $M(PMe_3)_4X_2$ and *trans*-$Ir(PPh_3)_2(CO)X$: strong π-donors favor addition to $M(PMe_3)_4X_2$ but disfavor addition to *trans*-$Ir(PPh_3)_2(CO)X$. The strikingly different effects that result from π-donation in these "16-electron" systems, $M(PMe_3)_4X_2$ and $Ir(PPh_3)_2(CO)X$, serve to emphasize the importance of considering the detailed nature of metal−ligand interactions in predicting and understanding the reactivity of a metal center. Thus, ancillary ligand variations do not necessarily influence a given reaction type (oxidative addition, in the present case) in the same way for different systems. The aforementioned common notion that electron-donating ligands promote oxidative addition reactions is, therefore, only likely to be universally true if σ effects are exclusively responsible for modifying the electron richness of a metal center.

The more facile oxidation of $M(PMe_3)_4X_2$ to $M(PMe_3)_4H_2X_2$ for the lighter halogens bears an interesting comparison with the electrochemical oxidation of the quadruply bonded dinuclear complexes $Mo_2X_4(PR_3)_4$ (X = Cl, Br, I), for which the ease of oxidation increases in the sequence I < Br < Cl.[54] The unexpected halide dependence was proposed to be a result of metal-to-halide back bonding, which serves to lower the energy of the δ and δ^* orbitals, an effect that should be greatest for the iodide derivative. An alternative possibility, however, which is more in line with the rationalization for the ease of oxidative addition of H_2 to $M(PMe_3)_4X_2$, is that the trend reflects the greater π-donor abilities of the lighter halogens, which serve to destabilize metal d orbitals more and thereby promote oxidation.

In addition to the influence of the halide ligand on the thermodynamics of the oxidative addition of H_2, the energetics of forming dihydrogen complexes has also been briefly described in the literature (Table 5). The situation with respect to $Ir(PR_3)_2H_2X$ derivatives, however, is conflicting. For example, Caulton has reported that addition of H_2 to $Ir(PBu^t_2Ph)_2H_2X$, giving the dihydrogen complexes $Ir(PBu^t_2Ph)_2H_2(\eta^2\text{-}H_2)X$, becomes more exothermically favored in the sequence Cl < Br < I.[41b,55] As with oxidative addition to the Vaska-type complexes, Caulton has concluded that π-donation by X stabilizes "16-electron" $Ir(PBu^t_2Ph)_2H_2X$, thereby resulting in H_2 addition being less exothermic than those in the absence of π-donation. In contrast to Caulton's $Ir(PBu^t_2Ph)_2H_2X$ system, Jensen has reported that the exothermicity of the closely related reaction of $Ir(PPr^i_3)_2H_2X$ with H_2 increases in the opposite sequence, i.e., I < Br < Cl.[56,57] At the same time, however, the "thermodynamic stabilization of the dihydrogen ligand", as judged by the equilibrium ratios of $Ir(PPr^i_3)_2H_2(\eta^2\text{-}H_2)X$:$Ir(PPr^i_3)_2H_2X$, has been noted to increase in the sequence, Cl < Br < I,[58,59] which *is* in accord with the equilibrium constant data for the $Ir(PBu^t_2Ph)_2H_2X$ system.[60,61]

An Inverse Equilibrium Isotope Effect for Oxidative Addition of H_2 to $W(PMe_3)_4I_2$. Rather surprisingly, the oxidative addition of H_2 to $W(PMe_3)_4I_2$ constitutes the first

(54) Zietlow, T. C.; Hopkins, M. D.; Gray, H. B. *J. Am. Chem. Soc.* **1986**, *108*, 8266−8267.

(55) For theoretical calculations on this system, see: Clot, E.; Eisenstein, O. *J. Phys. Chem. A* **1998**, *102*, 3592−3598.

(56) (a) Lee, D. W.; Jensen, C. M. *Inorg. Chim. Acta* **1997**, *259*, 359−362. (b) Lee, D. W.; Jensen, C. M. *J. Am. Chem. Soc.* **1996**, *118*, 8749−8750.

(57) Jensen has also noted that the exothermicity of the addition of H_2 to $Ir(PPr^i_3)_2H_2X$ in toluene solution is significantly less than that of the corresponding reaction in an alkane. Likewise, the entropy change for addition of H_2 is less negative in toluene than in an alkane. These observations have been proposed to be a result of arene solvation stabilizing each of the five-coordinate $Ir(PPr^i_3)_2H_2X$ species. Furthermore, the lower exothermicity for addition of H_2 to the iodide complex in alkane solvent with respect to that for the chloride and bromide has been suggested to indicate preferential alkane coordination to the five-coordinate iodide (ref 57).

(58) Le-Husebo, T.; Jensen, C. M. *Inorg. Chem.* **1993**, *32*, 3797−3798.

(59) Specifically, under H_2 (0.5 atm) at −80 °C, the reported $IrXH_2(\eta^2\text{-}H_2)(PPr^i_3)_2$:$IrXH_2(PPr^i_3)_2$ ratios are 0.56 (Cl), 0.91 (Br), and 1.67 (I).

(60) Furthermore, the $[Ir(\eta^2\text{-}H_2)]$ interaction in $Ir(PPr^i_3)_2H_2(\eta^2\text{-}H_2)X$ (X = Cl, Br, I) has been suggested to be strongest for the iodide derivative on the basis that the latter complex exhibits the highest barrier for rotation of the H_2 ligand [i.e., 0.98(5) kcal mol^{-1} for $Ir(PPr^i_3)_2H_2(\eta^2\text{-}H_2)I$, as compared to 0.51(2) kcal mol^{-1} for the chloride derivative]. See: Eckert, J.; Jensen, C. M.; Koetzle, T. F.; Husebo, T. L.; Nicol, J.; Wu, P. *J. Am. Chem. Soc.* **1995**, *117*, 7271−7272.

(61) A possible explanation for the discrepency of the $\Delta H°$ values for the two $Ir(PR_3)_2H_2(\eta^2\text{-}H_2)X$ systems may be associated with the equilibrium constant data having being measured over a relatively small temperature range.

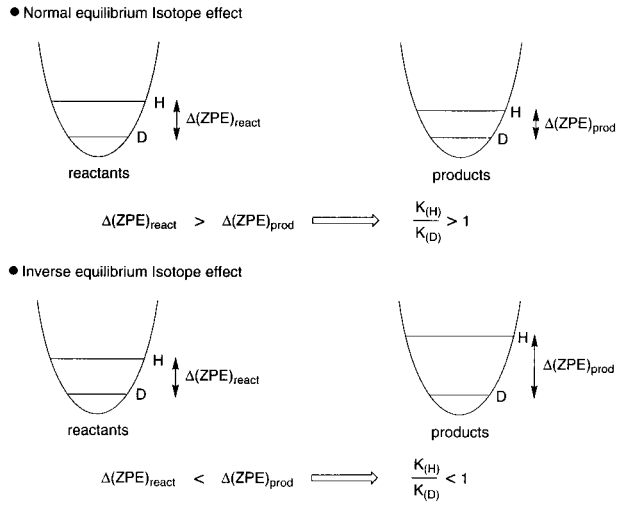

Figure 9. Normal and inverse equilibrium isotope effects.

literature report[3] of a system for which the equilibrium isotope effect for oxidative addition of H_2 to a transition metal complex was determined.[62,63] It is, therefore, noteworthy that the oxidative addition of D_2 to $W(PMe_3)_4I_2$ is characterized by a substantial *inverse* equilibrium deuterium isotope effect, with $K_H/K_D = 0.63(5)$ at 60 °C (Table 2). Prior to this example, the only other literature report of which we are aware is the composite primary and secondary equilibrium deuterium isotope for the oxidative addition of dihydrogen to $Cp_2Ta(\mu\text{-}CX_2)_2Ir(CO)(PPh_3)$ (X = H, D).[64] For this latter system, however, rapid deuterium exchange into the $[Ta(\mu\text{-}CH_2)_2Ir]$ methylene groups prevented determination of the primary effect.[65]

The inverse nature of the deuterium equilibrium isotope effect (i.e., $K_H/K_D < 1$) for oxidative addition of H_2 is particularly interesting since it is completely counter to that which would have been predicted on the basis of the simple notion concerning primary isotope effects, namely that deuterium prefers to reside in the stronger bond (i.e., the higher energy oscillator). Thus, with a D−D bond which is 1.8 kcal mol^{-1} stronger than the H−H bond,[14] a normal (i.e., $K_H/K_D > 1$) equilibrium isotope effect may have been predicted for the oxidative addition of H_2 to a transition metal complex (Figure 9). For example, the equilibrium between a dihydride $[MH_2]$ and a dihydrogen $[M(\eta^2\text{-}H_2)]$ complex was argued to be inverse on the basis of the notion that M−H (M−D) bonds are weaker than H−H (D−D) bonds.[66,67] Furthermore, solid-state metal deuterides are normally less stable than the corresponding hydrides with respect to elimination of D_2 (H_2) due to the greater D−D versus H−H bond energy.[68] With this perspective, the inverse nature of the deuterium equilibrium isotope effect for oxidative addition of H_2 to $W(PMe_3)_4I_2$ must be regarded as counterintuitive. However, it is now apparent that the occurrence of an inverse deuterium equilibrium isotope effect for addition of H_2 to a single transition metal center (be it the formation of a dihydride or dihydrogen complex) is a rather general phenomenon (Table 6).[69]

The temperature dependence of K reveals that the origin of the inverse equilibrium deuterium isotope effect is enthalpic, with oxidative addition of D_2 being more exothermic than oxidative addition of H_2 [$\Delta H°_D = -21.6(7)$ kcal mol^{-1} versus $\Delta H°_H = -19.7(6)$ kcal mol^{-1}]. As a consequence, the W−D bond is substantially stronger than the W−H bond [D(W−D) = 63.8(7) kcal mol^{-1} versus D(W−H) = 62.0(6) kcal mol^{-1}]. The entropic contribution to the equilibrium isotope effect is small [$\Delta S°_D = -51(3)$ eu versus $\Delta S°_H = -45(2)$ eu] but actually attempts to counter the inverse nature. The source of this small difference in $\Delta S°$ for the oxidative addition of H_2 and D_2 is presumably the greater entropy of D_2 compared to that of H_2 (39.0 and 34.0 eu, respectively, at 300 K).[70] Examination of the data in Table 6 indicates that the inverse equilibrium isotope effects observed in other systems are also due to an enthalpic influence (i.e., $\Delta H°_H - \Delta H°_D > 0$), with the small entropic contributions attempting to counter the effect and favor addition of H_2, i.e., $\Delta S°_H - \Delta S°_D > 0$.

The interpretation of equilibrium isotope effects is normally discussed in terms of four factors, namely SYM (a symmetry number factored out of the rotational partition function ratio), MMI (a mass and moment of inertia contribution due to changes in rotational and translational motion), EXC (an excitation contribution accounting for population of vibrational levels), and ZPE (a zero point energy term).[71,72] Of these terms, SYM,

$$\text{EIE} = \text{SYM}\cdot\text{MMI}\cdot\text{EXC}\cdot\text{ZPE}$$

MMI, and EXE relate to the entropy of the EIE, while ZPE provides the major contribution for the enthalpy. Most commonly, the ZPE term is considered to dominate the EIE, which

(62) The equilibrium deuterium isotope effect for the oxidative addition of H_2 to *trans*-$Ir(PPh_3)_2(CO)Cl$ has been reported: Werneke, M. F. Ph.D Thesis, Clarkson College of Technology, Potsdam, NY, 1971.

(63) For reviews of isotope effects in reactions of transition metal hydrides, see: (a) Bullock, R. M. In *Transition Metal Hydrides*; Dedieu, A., Ed.; VCH: New York, 1992; pp 263−307. (b) Rosenberg, E. *Polyhedron* **1991**, *8*, 383−405.

(64) Hostetler, M. J.; Bergman, R. G. *J. Am. Chem. Soc.* **1992**, *114*, 7629−7636.

(65) The deuterium equilibrium isotope effect for addition of Et_3SiH to $Cp_2Ta(\mu\text{-}CH_2)_2Ir(CO)(PPh_3)$ has also been shown to be inverse, ranging from 0.53 ± 0.04 at 0 °C to 0.77 ± 0.06 at 60 °C. As with addition of H_2, these values also are a composite of primary and secondary effects. However, for this particular system, the primary and secondary isotope contributions were estimated to be 0.73 and 0.74, respectively, on the basis of IR calculations for the primary effect. See ref 64.

(66) (a) Packett, D. L.; Trogler, W. C. *J. Am. Chem. Soc.* **1986**, *108*, 5036−5038. (b) Packett, D. L.; Trogler, W. C. *Inorg. Chem.* **1988**, *27*, 1768−1775. (c) Howarth, O. W.; McAteer, C. H.; Moore, P.; Morris, G. E. *J. Chem. Soc., Dalton Trans.* **1984**, 1171−1180. (d) Reference 1a, p 331.

(67) Other examples which support this notion include the observations that the heavier isotope (^2H or ^3H) favors the dihydrogen site in (i) $[Re(PMe_2Ph)_3(CO)(\eta^2\text{-}H_2)H_2]^+$ [a] and (ii) $CpNb(CO)_3(\eta^2\text{-}H_2)$ versus $CpNb(CO)_3H_2$.[b] Furthermore, an inverse kinetic isotope effect for reductive elimination of H_2 from *cis*-$Pt(PMe_3)_2H_2$ has been interpreted in terms of a preequilibrium with *cis*-$Pt(PMe_3)_2(\eta^2\text{-}H_2)$ in which deuterium prefers to be located in the dihydrogen species.[c] However, more recent work indicates that this prediction is oversimplified, with several counter examples having been reported. Thus, the heavier isotope favors the hydride sites in $[Tp^{RR'}]Ir(PR_3)(\eta^2\text{-}H_2)H]^+$ [d,e] and $[Cp_2W(\eta^2\text{-}H_2)H]^+$.[f] Furthermore, using assumed values for the EIE for coordination of H_2 and for oxidative addition of H_2 in a hypothetical system, the heavier isotopomer has been predicted to favor the terminal hydride site.[g] It is, therefore, evident that the factors which influence the preference for deuterium (or tritium) to occupy either a hydride or dihydrogen site are complex. (a) Luo, X-L.; Crabtree, R. H. *J. Am. Chem. Soc.* **1990**, *112*, 6912−6918. (b) Haward, M. T.; George, M. W.; Hamley, P.; Poliakoff, M. *J. Chem. Soc., Chem. Commun.* **1991**, 1101−1103. (c) Packett, D. L.; Trogler, W. C. *Inorg. Chem.* **1988**, *27*, 1768−1775. (d) Heinekey, D. M.; Oldham, W. J., Jr. *J. Am. Chem. Soc.* **1994**, *116*, 3137−3138. (e) Oldham, W. J., Jr.; Hinkle, A. S.; Heinekey, D. M. *J. Am. Chem. Soc.* **1997**, *119*, 11028−11036. (f) Henderson, R. A.; Oglieve, K. E. *J. Chem. Soc., Dalton Trans.* **1993**, 3431−3439. (g) Bender, B. R.; Kubas, G. J.; Jones, L. H.; Swanson, B. I.; Eckert, J.; Capps, K. B.; Hoff, C. D. *J. Am. Chem. Soc.* **1997**, *119*, 9179−9190.

(68) However, in some instances, e.g., VH_2, NbH_2, $(V,Nb)H_2$, and $LaNi_5H_6$, the deuterides are more stable. See: (a) Wiswall, R. H., Jr.; Reilly, J. J. *Inorg. Chem.* **1972**, *11*, 1691−1696. (b) Luo, W.; Clewley, J. D.; Flanagan, T. B. *J. Phys. Chem.* **1990**, *93*, 6710−6722.

(69) An exception appears to be binuclear oxidative addition of H_2, which has recently been reported to exhibit a normal equilibrium isotope effect. See ref 51g.

Table 6. Deuterium Equilibrium Isotope Effects for Addition of H_2 to Transition Metal Complexes[a]

reactant	product	K_H/K_D	$\Delta H°_H$, $\Delta H°_D$	$\Delta S°_H$, $\Delta S°_D$	$\Delta H°_H - \Delta H°_D$	$\Delta S°_H - \Delta S°_D$	refs
$W(PMe_3)_4I_2$	$W(PMe_3)_4H_2I_2$	0.63(5) at 60 °C	−19.7(6), −21.6(7)	−45(2), −51(3)	1.9(1.3)	6(5)	this work
$Ir(PCy_3)_2HCl_2$	$Ir(PCy_3)_2H(\eta^2\text{-}H_2)Cl$	0.50 at −13 °C					b
$Ir(PBu^t_2Me)_2H_2Cl$	$Ir(PBu^t_2Me)_2H_2(\eta^2\text{-}H_2)Cl$	0.37 at -13 °C	−6.8(2), −7.7(5)	−19.2(7), −20.7(1.8)	0.9	1.5	41b
$Cr(CO)_3(PCy_3)_2$	$Cr(CO)_3(PCy_3)_2(\eta^2\text{−}H_2)$	0.65(15) at 22 °C	−6.8(5), −8.6(5)	−24.7(2.0), −30.0(2.0)	1.8	5.3	67g
$W(CO)_3(PCy_3)_2(N_2)$	$W(CO)_3(PCy_3)_2(\eta^2\text{-}H_2)$	0.70(15) at 22 °C					67g
$Os(PPr^i_3)_2(CO)(Cl)H$	$Os(PPr^i_3)_2(CO)\text{-}(Cl)H(\eta^2\text{-}H_2)$	0.35 at 85°C	−14.1(5), −14.8	−30(1), −30	0.7	0	c
$Ru(PPr^i_3)_2(CO)(Cl)H$	$Ru(PPr^i_3)_2(CO)(Cl)H(\eta^2\text{-}H_2)$		−7.7(2)	−23.2(1.0)			d
$Ir(PPh_3)_2(CO)Cl$	$Ir(PPh_3)_2(CO)ClH_2$	0.47 at 30 °C	−14.4(8) −14.8(8)	−26.0(2.4) −28.0(2.3)	0.8	2.0	e
$Cp_2Ta(\mu\text{-}CH_2)_2Ir(CO)\text{-}(PPh_3)$	$Cp_2Ta(\mu\text{-}CH_2)_2IrH_2(CO)\text{-}(PPh_3)$	0.54(4) at 22 °C	−12.0(2), −13.0(4)	−23.7(6), −25.9(1.2)	1.0(6)	2.2(1.8)	64

[a] The equilibrium isotope effects for reactions involving $Ir(PCy_3)_2HCl_2$, $Ir(PBu^t_2Me)_2H_2Cl$, $Os(PPr^i_3)_2(CO)(Cl)H$, and $Cp_2Ta(\mu\text{-}CH_2)_2Ir(CO)(PPh_3)$ are complicated by secondary isotope effects due to deuterium exchange into the hydride sites. Furthermore, the value for $W(CO)_3(PCy_3)(N_2)$ is for net binding and does not distinguish between dihydride and dihydrogen forms. [b] Gusev, D. G.; Bakhmutov, V. I.; Grushin, V. V.; Vol'pin, M. E. *Inorg. Chim. Acta* **1990**, *177*, 115−120. [c] Bakhmutov, V. I.; Bertrán, J.; Esteruelas, M. A.; Lledós, A.; Maseras, F.; Modrego, J.; Oro, L. A.; Sola, E. *Chem. Eur. J.* **1996**, *2*, 815−825. Values for deuterated system calculated from the data presented in this reference. [d] Gusev, D. G.; Vymenits, A. B.; Bakhmutov, V. I. *Inorg. Chem.* **1992**, *31*, 2−4. [e] Reference 62, pp 187 and 239. A value of 0.55(6) at 22 °C is reported in Abu-Hasanayn, F.; Krogh-Jespersen, K.; Goldman, A. S. *J. Am. Chem. Soc.* **1993**, *115*, 8019−8023.

is the reason why it is normally expected that the isotopomer with deuterium located in the site with the highest vibrational frequency is the most stable. Specifically, for a diatomic molecule, the difference in zero point energies, $\Delta E° = \epsilon°_H - \epsilon°_D$, is directly proportional to the square of the force constant (k),[73] such that $\Delta\epsilon°$ increases with vibrational frequency. As a consequence, the zero point energy stabilization for a system is greatest when deuterium resides in the highest energy oscillator; i.e., deuterium prefers to reside in the stronger bond (Figure 9). As is evident from the above discussion, an inverse equilibrium deuterium isotope effect for oxidative addition to $W(PMe_3)_4I_2$ would *not* have been predicted by consideration of the zero point energy differences associated with the observed W−H and W−D *stretching* frequencies alone. Specifically, the observed ν_{W-H} and ν_{W-D} stretching frequencies of 1961 and 1416 cm^{-1} in $W(PMe_3)_4H_2I_2$ and $W(PMe_3)_4D_2I_2$, respectively, result in a zero point energy difference of 273 cm^{-1} for this vibrational mode. If the symmetric and asymmetric stretches have similar frequencies, then the combined zero point energy lowering would be less than the difference between D_2 and H_2 zero point energies (630 cm^{-1}),[74] so that a normal equilibrium isotope effect would have been predicted. To rationalize the enthalpic origin of the inverse primary equilibrium isotope effect, it is important to consider *bending* modes associated with the dihydride moiety, modes that are not normally invoked when discussing *primary*[75] isotope effects due to their low energy.[76] However, even though bending modes are of low energy, the fact that there are *four*[77] such modes associated with the $[WH_2]$ moiety (Figure 10) means that, in combination, they may provide an important contribution. Thus, inclusion of the bending modes results in a significant lowering of the zero point energy for $W(PMe_3)_4D_2I_2$ with respect to $W(PMe_3)_4H_2I_2$, to the extent that

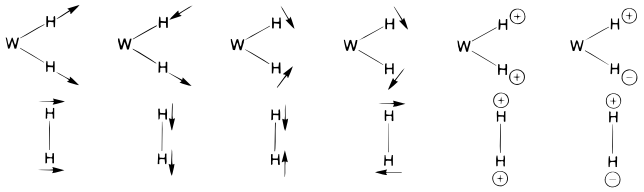

Figure 10. Vibrational modes associated with a $[MH_2]$ moiety.

an inverse equilibrium isotope effect may result. For example, assuming a value of 600 cm^{-1} for each of the four $[WH_2]$ deformations,[76] and a corresponding value of ca. 425 cm^{-1} for $[WD_2]$, each of the bending modes would contribute a difference of ca. 175 cm^{-1} to the difference in zero point energies of $W(PMe_3)_4H_2I_2$ and $W(PMe_3)_4D_2I_2$, so that the total difference would be ca. 923 cm^{-1}, rather than the 223 cm^{-1} predicted by consideration of the W−H(D) stretching frequencies alone. Since this difference of 923 cm^{-1} in zero point energies is greater than that between D_2 and H_2 (630 cm^{-1}), an inverse deuterium equilibrium isotope effect will result (Figure 9). Theoretical calculations support such a notion, with the ZPE level of $W(PMe_3)_4D_2I_2$ calculated to be 1049 cm^{-1} (3.0 kcal mol^{-1})[78] lower than that of $W(PMe_3)_4H_2I_2$. At 60 °C, the oxidative addition of D_2 to $W(PMe_3)_4I_2$ is calculated to be 0.86 kcal mol^{-1} more exothermic than that of H_2,[79] and the EIE is predicted to be 0.73, in favorable agreement with the experimental value of 0.63(5).

(70) Wooley, H. W.; Scott, R. B.; Brickwedde, F. G. *J. Res. Nat. Bur. Stand.* **1948**, *41*, 379−475.

(71) Abu-Hasanayn, F.; Krogh-Jespersen, K.; Goldman, A. S. *J. Am. Chem. Soc.* **1993**, *115*, 8019−8023.

(72) McLennan, D. J. In *Isotopes in Organic Chemistry*; Buncel, E., Lee, C. C., Eds.; Elsevier: New York, 1987; Vol 7, Chapter 6, pp 393−480.

(73) Specifically, $\Delta\epsilon° = A(k)^{1/2}$, where $A = [(h/4\pi)(1 - 0.5^{1/2})]$. The latter equation assumes an X−H harmonic oscillator [i.e., $\epsilon° = (1/2)h\nu$; $\nu = (1/2\pi)(k/\mu)^{1/2}$], where X is heavy, such that $\mu = m_H$ and m_D. See ref 72.

(74) $\nu_{H-H} = 4395$ cm^{-1}; $\nu_{D-D} = 3118$ cm^{-1}. See: Herzberg, G. *Molecular Spectra and Molecular Structure*; Van Nostrand Reinhold Co.: New York, 1950; Vol. 1, pp 532−533.

(75) It is, however, important to consider bending modes in evaluating secondary isotope effects.

(76) Relatively little information is available concerning the bending modes associated with transition metal hydride complexes, although the bending modes in $Mo(PR_3)_4H_4$ derivatives are observed in the range 600−800 cm^{-1}.[a] Similar values have also been suggested and calculated for other systems.[b−e] (a) Polyakova, V. B.; Borisov, A. P.; Makhaev, V. D.; Semenenko, K. D. *Koord. Khim.* **1980**, *6*, 743−752. (b) Girling, R. B.; Grebenik, P.; Perutz, R. N. *Inorg. Chem.* **1986**, *25*, 31−36. (c) Macgregor, S. A.; Eisenstein, O.; Whittlesey, M. K.; Perutz, R. N. *J. Chem. Soc., Dalton Trans.* **1998**, 291−300. (d) Reference 67g. (e) Jonas, V.; Thiel, W. *J. Chem. Phys.* **1996**, *105*, 3636-3648. (f) Egdell, W. F.; Fisher, J. W.; Asato, G.; Risen, W. M., Jr. *Inorg. Chem.* **1969**, *8*, 1103−1108. (g) Sweany, R. L.; Russell, F. N. *Organometallics* **1988**, *7*, 719−727.

(77) These modes are derived from the lost translational and rotational degrees of freedom for H_2.

(78) ZPE of $W(PMe_3)_4H_2I_2 = 296.141$ kcal mol^{-1}; ZPE of $W(PMe_3)_4D_2I_2 = 293.129$ kcal mol^{-1}.

(79) At 60 °C, $H[W(PMe_3)_4I_2] = -1\,214\,192.67$ kcal mol^{-1}, $H[W(PMe_3)_4H_2I_2] = -1\,214\,926.98$ kcal mol^{-1}, $H[W(PMe_3)_4D_2I_2] = -1\,214\,929.68$ kcal mol^{-1}, $H[H_2] = -731.79$ kcal mol^{-1}, $H[D_2] = -733.63$ kcal mol^{-1}; $S[W(PMe_3)_4I_2] = 184.17$ eu, $S[W(PMe_3)_4H_2I_2] = 205.17$ eu, $S[W(PMe_3)_4D_2I_2] = 206.62$ eu, $S[H_2] = 31.90$ eu, $S[D_2] = 35.31$ eu

In essence, the occurrence of an inverse deuterium equilibrium isotope effect is a consequence of there being a *single* isotope-sensitive vibrational mode in the reactant (H_2) yet *six* (albeit lower energy) isotope-sensitive modes in the product. It is because of this peculiar situation with respect to the large difference in *number* of isotope-sensitive modes for addition of H_2 that the observed isotope effect becomes counterintuitive: in all other examples of primary equilibrium isotope effects there is not such a large difference in the number of isotope-sensitive modes, and so the magnitude and direction of the isotope effect is governed principally by the relative strengths of the bonds broken and formed.[80]

A more detailed analysis of the origin of the inverse equilibrium isotope effect has recently been provided by Krogh-Jespersen and Goldman for addition of H_2 to Vaska's complex.[71] Specifically, Krogh-Jespersen and Goldman have calculated that the combination of the three entropy-determining contributions of SYM (1.0), MMI (5.66), and EXC (0.84) result in a normal contribution to the EIE (i.e., a positive value of $\Delta S°_H - \Delta S°_D$), and that the inverse nature of the EIE is essentially a consequence of a dominant zero point energy term, with ZPE = 0.10, resulting in a positive value of $\Delta H°_H - \Delta H°_D$.[81] That the four bending modes are responsible for the inverse nature of the EIE is further indicated by the fact that eliminating them from the calculation results in the prediction of a normal EIE of 4.6. Using a similar approach, we have used the calculated isotope-sensitive vibrational frequencies of $W(PMe_3)_4H_2I_2$ to predict an EIE of 0.73 at 60 °C,[82,83] which is identical to the value of 0.73 predicted by the complete energy calculation described above. As with the Vaska system, the inverse nature of the EIE is the result of a dominant zero point energy term: ZPE (0.17), MMI (5.25), and EXC (0.80).[83]

Bender, Kubas, Hoff, and co-workers have also considered the origin of inverse deuterium equilibrium isotope effects in the formation of dihydrogen complexes. Specifically, calculations analogous to those of Krogh-Jespersen and Goldman described above revealed that the observed isotope effect [$K_H/K_D = 0.70(15)$ at 22 °C] for the formation of $W(CO)_3(PCy_3)_2(\eta^2\text{-}H_2)$ from $W(CO)_3(PCy_3)_2(N_2)$ is primarily attributable to an inverse zero point energy factor (0.20), with a smaller contribution from the vibrational excitation factor (0.67); as with oxidative addition of H_2, the MMI factor is large and normal (5.77). Furthermore, as with full oxidative addition, analysis of the zero point energy components indicates that the inclusion of all six [WH_2] vibrational modes is essential to obtaining an inverse deuterium EIE.

Mechanism of Oxidative Addition and Reductive Elimination of H_2. Kinetics studies have allowed details of the mechanism of the oxidative addition/reductive elimination transformation to be elucidated. In particular, these studies demonstrate that $W(PMe_3)_4H_2I_2$ is not obtained by the direct oxidative addition of H_2 to six-coordinate *trans*-$W(PMe_3)_4I_2$ but rather occurs via initial dissociation of PMe_3. For example, the rate of oxidative addition is strongly inhibited by addition of PMe_3, so that a mechanism involving PMe_3 dissociation and a five-coordinate [$W(PMe_3)_3I_2$] intermediate is implied (Scheme 2).[84] Further support for a mechanism involving rate-determining dissociation of PMe_3 is provided by the observation that there is no deuterium kinetic isotope effect for addition of D_2 to *trans*-$W(PMe_3)_4I_2$; however, a deuterium kinetic isotope effect *is* observed in the presence of PMe_3 (Figure 11), under which conditions addition of PMe_3 to the five-coordinate [$W(PMe_3)_3I_2$] intermediate becomes competitive with oxidative addition of H_2.

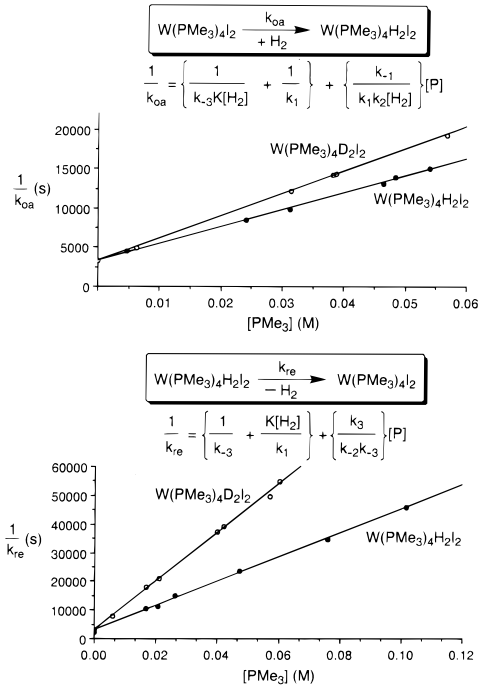

Figure 11. Variation of k_{oa} and k_{re} with [PMe_3].

Scheme 2. Proposed Mechanism for Oxidative Addition of H_2 to $W(PMe_3)_4I_2$

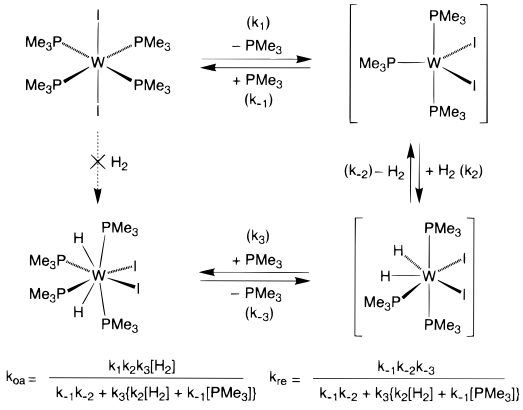

(80) For example, the deuterium equilibrium isotope effect for oxidative addition of Me−H versus Me−D is calculated to be normal since the reactant and product have the same number of isotope-sensitive modes and C−H bonds are stronger than M−H bonds. See: Abu-Hasanayn, F.; Krogh-Jespersen, K.; Goldman, A. S. *J. Am. Chem. Soc.* **1993**, *115*, 8019−8023.

(81) As a result of the difference in symmetry number between [MH_3] and [*cis*-HMD_2] moieties, Goldman and Krogh-Jespersen have predicted an even more pronounced inverse equilibrium isotope effect of 0.33 for oxidative addition to $M(PR_3)_2(CO)H$. The difference in symmetry number arises from the fact that, for statistical reasons, elimination of H_2 from [MH_3] is twice as fast as elimination of D_2 from [*cis*-HMD_2]. Such a symmetry effect would not, however, be operative for an equilibrium involving [*trans*-HMD_2]. See ref 80.

(82) Calculated vibrational frequencies (cm^{-1}) for $W(PMe_3)_4H_2I_2$: 1991, 1987, 1102, 837, 759, 649. Calculated vibrational frequencies (cm^{-1}) for $W(PMe_3)_4D_2I_2$: 1419, 1411, 782, 609, 549, 464. The experimental values of 4395 and 3118 cm^{-1} were used for H2 and D_2.

(83) MMI, EXC, and ZPE terms were determined from the calculated vibrational frequencies using a program provided by Dr. Bruce Bender.

(84) On its own, the observation of inhibition by PMe_3 can also be rationalized by formation of a seven-coordinate species $W(PMe_3)_5I_2$, which serves to reduce the concentration of six-coordinate $W(PMe_3)_4I_2$. However, such a species is not observed by ^1H NMR spectroscopy. Furthermore, if inhibition were a result of forming $W(PMe_3)_5I_2$, a kinetic isotope effect in the absence of added PMe_3 would have been expected. In contrast, the kinetic isotope effect is observed only in the presence of PMe_3 (see text).

As implied by microscopic reversibility, the reductive elimination of H_2 from $W(PMe_3)_4H_2I_2$ must also proceed via initial PMe_3 dissociation. Accordingly, the reductive elimination of H_2 from $W(PMe_3)_4H_2I_2$ is also inhibited by the presence of PMe_3, and a deuterium kinetic isotope effect is observed only in the presence of added PMe_3 (Figure 11).

Prior dissociation of PMe_3 in the oxidative addition and reductive elimination reactions of $W(PMe_3)_4I_2$ and $W(PMe_3)_4H_2I_2$ has literature precedence.[85] For example, the principal pathway for hydrogenation of Wilkinson's catalyst, $Rh(PPh_3)_3Cl$, giving $Rh(PPh_3)_3H_2Cl$, involves initial dissociation of PPh_3.[86] Thus, under normal conditions, the rate of the reaction is limited by phosphine dissociation and is consequently independent of H_2 concentration; only in the presence of excess PPh_3 does the direct pathway become significant. Despite these observations, however, it is important to emphasize that initial ligand dissociation is not a required step for all oxidative addition and reductive elimination reactions involving H_2. Indeed, oxidative addition and reductive elimination reactions involving H−H, C−H, and C−C bonds may proceed either directly or via sequences involving either (i) prior ligand loss or (ii) prior ligand addition.[85]

It is, therefore, evident there must be a rather subtle interplay of factors which influence whether oxidative addition and reductive elimination occur directly or via prior ligand dissociation or addition. Nevertheless, a simple (perhaps oversimplified) rationalization as to why $W(PMe_3)_4H_2I_2$ undergoes PMe_3 dissociation prior to reductive elimination of H_2 is associated with the notion that the strong σ-donor PMe_3 ligand stabilizes high valence states. As such, reductive elimination of H_2 would be promoted by prior loss of PMe_3. It is also possible that the lower coordination number may allow for more facile structural reorganization that accompanies the *cis*-to-*trans* rearrangement.

Kinetic Isotope Effects for Oxidative Addition and Reductive Elimination. A detailed study of the kinetics of the oxidative addition and reductive elimination transformations has allowed the free energy surface illustrated in Figure 12 to be established. It is likely that dihydrogen species,[87] for example $[W(PMe_3)_3(\eta^2\text{-}H_2)I_2]$ and $[W(PMe_3)_4(\eta^2\text{-}H_2)I_2]$, may also be intermediates on the energy surface, but since our data are not capable of providing support either for or against such species as intermediates (as opposed to transition states), we have excluded them from the analysis. The primary kinetic deuterium isotope effect for the oxidative addition step of H_2 to $[W(PMe_3)_3I_2]$ is $k_{2(H)}/k_{2(D)} = 1.2(2)$ at 60 °C (Table 7).[63] While such a value is small, it is in accord with previous studies, as illustrated in Table 8.[88,89] In view of the large difference in zero point energies of H_2 versus D_2 (due to the strong nature of the bonds), low values for deuterium kinetic isotope effects have previously been invoked as an indication of an early transition state (i.e., little H−H bond cleavage);[29b,90] however, recent work suggests that such interpretation may be greatly oversimplified. Kinetic isotope effects may be considered to be a product of three terms,

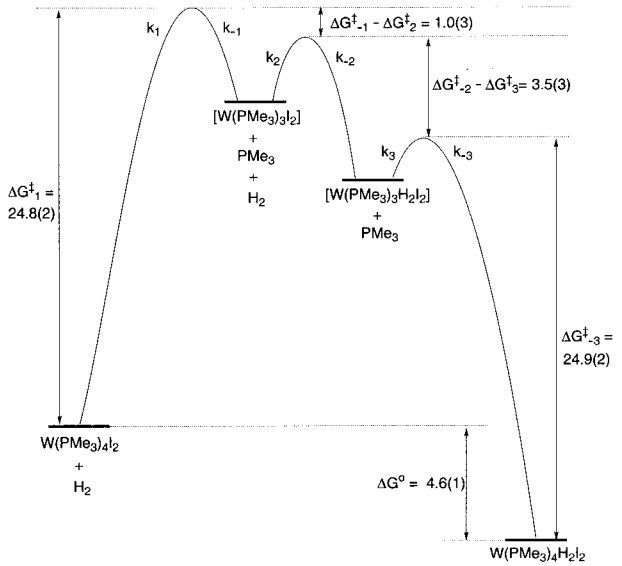

Figure 12. Free energy surface for oxidative addition of H_2 to $W(PMe_3)_4I_2$.

Table 7. Kinetic Isotope Effects for Oxidative Addition of H_2 and D_2 to $W(PMe_3)_4I_2$

	k_1 (s^{-1})	k_2/k_{-1}	k_{-2}/k_3 (M^{-1})	k_{-3} (s^{-1})
k_H	$3.91(40) \times 10^{-4}$	4.3(1.7)	$5.4(1.7) \times 10^{-3}$	$3.38(40) \times 10^{-4}$
k_D	$3.68(40) \times 10^{-4}$	3.7(1.3)	$2.7(10) \times 10^{-3}$	$3.25(40) \times 10^{-4}$
k_H/k_D	1.00[a]	1.2(2)	2.0(2)	1.0(1)

[a] Since neither product nor reactant incorporates deuterium, an isotope effect does not exist.

Table 8. Kinetic Deuterium Isotope Effects for Addition and Elimination of H_2 to Transition Metal Complexes

reactant	product	k_H/k_D	ref
	Addition of H_2		
$[W(PMe_3)_3I_2]$	$[W(PMe_3)_3H_2I_2]$	1.2(2) at 60 °C	this work
$[Cr(CO)_5(C_6H_{12})]$	$Cr(CO)_5(\eta^2\text{-}H_2)$	1.9 at 23 °C	*a*
$[Rh(PPh_3)_2Cl]$	$Rh(PPh_3)_2H_2Cl$	1.5 at 23 °C	*b*
$[Fe(CO)_4]$	$[Fe(CO)_4H_2]$	1.1(1) at 24 °C	*c*
$Ir(PPh_3)_2(CO)Cl$	$Ir(PPh_3)_2(CO)ClH_2$	1.09 at 25 °C	*d*
	Elimination of H_2		
$[W(PMe_3)_3H_2I_2]$	$[W(PMe_3)_3I_2]$	2.0 at 60 °C	this work
$W(CO)_3(PPh_3)_2(H_2)$	$W(CO)_3(PPh_3)_2(py)$	1.7 (15−35 °C)	*c*
$Cr(CO)_5(\eta^2\text{-}H_2)$	$[Cr(CO)_5]$	5.0 at 23 °C	*a*
cis-$Pt(PMe_3)_2H_2$	[*cis*-$Pt(PMe_3)_2$]	0.45(1) at 21 °C	*f*

[a] $[Cr(CO)_5(C_6H_{12})]$ was generated by photolysis of $Cr(CO)_6$ in cyclohexane. See: Church, S. P.; Grevels, F.-W.; Hermann, H.; Schaffner, K. *J. Chem. Soc., Chem. Commun.* **1985**, 30−32. [b] $[Rh(PPh_3)_2Cl]$ was generated by photolysis of $Rh(PPh_3)_2(CO)Cl$. See: Wink, D. A.; Ford, P. C. *J. Am. Chem. Soc.* **1987**, *109*, 436−442. [c] Wang, W.; Narducci, A. A.; House, P. G.; Weitz, E. *J. Am. Chem. Soc.* **1996**, *118*, 8654−8657. [d] (a) Zhou, P.; Vitale, A. A.; San Filippo, J., Jr.; Saunders, W. H., Jr. *J. Am. Chem. Soc.* **1985**, *107*, 8049−8054 and references therein. (b) Abu-Hasanayn, F.; Krogh-Jespersen, K.; Goldman, A. S. *J. Am. Chem. Soc.* **1993**, *115*, 8019−8023. (c) $\Delta H^{\ddagger}_H = 10.6$ kcal mol^{-1}, $\Delta H^{\ddagger}_D = 11.0$ kcal mol^{-1}; $\Delta S^{\ddagger}_H = -24.4$ eu, $\Delta S^{\ddagger}_D = -23.2$ eu. [e] Zhang, K.; Gonzalez, A. A.; Hoff, C. D. *J. Am. Chem. Soc.* **1989**, *111*, 3627−3632. [f] Packett, D. L.; Trogler, W. C. *Inorg. Chem.* **1988**, *27*, 1768−1775.

(85) For a listing of oxidative addition and reductive elimination reactions that involve either direct addition or elimination, or a mechanism involving initial dissociation or addition of a ligand, see Table S6 in the Supporting Information.

(86) (a) Halpern, J.; Wong, C. S. *J. Chem. Soc., Chem. Commun.* **1973**, 629−630. (b) Halpern, J.; Okamoto, T.; Zakhariev, A. *J. Mol. Catal.* **1976**, *2*, 65−68. (c) Halpern, J. *Inorg. Chim. Acta* **1981**, *50*, 11−19.

(87) (a) Heinekey, D. M.; Oldham, W. J., Jr. *Chem. Rev.* **1993**, *93*, 913−926. (b) Crabtree, R. H. *Acc. Chem. Res.* **1990**, *23*, 95−101. (c) Jessop, P. G.; Morris, R. H. *Coord. Chem. Rev.* **1992**, *121*, 155−284. (d) Crabtree, R. H. *Angew. Chem., Int. Ed. Engl.* **1993**, *32*, 789−805. (e) Kubas, G. J. *Acc. Chem. Res.* **1988**, *21*, 120−128.

(88) Kinetic deuterium isotope effects for a three-centered transition state are greatest for a symmetric transition state and decrease for transition states that are either product-like or reactant-like; indeed, calculations indicate that the isotope effect could become inverse (<1) in certain situations. See: (a) Bigeleisen, J. *Pure Appl. Chem.* **1964**, *8*, 217−222. (b) Melander, L. *Acta Chem. Scand.* **1971**, *25*, 3821−3826. (c) More O'Ferrall, R. A. *J. Chem. Soc. (B)* **1970**, 787−790. (d) Bigeleisen, J.; Wolfsberg, M. *Adv. Chem. Phys.* **1958**, *1*, 15−76.

(89) *Hydride* transfer from a transition metal hydride to $[Ph_3C]^+$ is known to be characterized by both normal and inverse kinetic isotope effects. See: Cheng, T.-Y.; Bullock, R. M. *J. Am. Chem. Soc.* **1999**, *121*, 3150−3155.

i.e., KIE = MMI·EXC·ZPE, and Goldman and Krogh-Jespersen have demonstrated that the observed small deuterium kinetic isotope effect for addition of H_2 to Vaska's complex, $Ir(PPh_3)_2(CO)Cl$, is a result of a large normal MMI term (5.66) being compensated by inverse values for EXC (0.57) and ZPE (0.38), which yield a calculated KIE of 1.23.[41a,90] As with the equilibrium isotope effects described above, the origin of the inverse values for EXC and ZPE may be attributed to the difference between both the number and magnitude of isotope-sensitive modes in the reactants and transition state. Thus, the activated complex has *five* isotope-sensitive modes that are orthogonal to the reaction coordinate, whereas the reactant (H_2) has only a single (albeit higher energy) vibration, thereby resulting in an inverse ZPE term. Furthermore, since the isotope-sensitive modes in the transition state are of low energy, there will be a significant difference in the occupation of excited vibrational states for the deuterio versus protio activated complex. By comparison, the difference in occupation of excited vibrational states for H_2 and D_2 is small due to the high vibrational frequency of their bonds, and so an inverse value for EXC results.

In contrast to the kinetic isotope effect for oxidative addition, that for reductive elimination of H_2 from $[W(PMe_3)_3H_2I_2]$ (k_{-2}) cannot be determined directly, since only the ratio k_{-2}/k_3 can be measured. However, on the basis that the secondary isotope effect for addition of PMe_3 to $[W(PMe_3)_3H_2I_2]$ is expected to be negligible (i.e., $k_{3(H)}/k_{3(D)} \approx 1$), the kinetic isotope effect for the reductive elimination step may be estimated as $k_{-2(H)}/k_{-2(D)} \approx 2$ at 60 °C. Such a value is comparable to other values for reductive elimination (Table 8) and is completely in accord with the inverse equilibrium isotope effect; i.e., an inverse equilibrium isotope effect for addition of H_2 merely implies that the kinetic isotope effect for reductive elimination is greater than that for oxidative addition.

Summary

In conclusion, experimental and theoretical studies indicate that the exothermicity of the oxidative addition of H_2 to the six-coordinate molybdenum and tungsten complexes $M(PMe_3)_4X_2$ (M = Mo, W; X = F, Cl, Br, I) increases in the sequences Mo < W and I < Br < Cl < F. The observed halogen dependence is most interesting since it provides a striking contrast to that reported for oxidative addition of H_2 to *trans*-$Ir(PPh_3)_2(CO)X$. Theoretical studies suggest that the halide dependence for $M(PMe_3)_4X_2$ is a result of both steric and electronic factors. Thus, sterically, oxidative addition is favored most for the fluoride derivatives, since the increased steric interactions upon forming the eight-coordinate complexes $M(PMe_3)_4H_2X_2$ would be minimized for the smaller halogen. Electronically, oxidative addition is favored most for the fluoride derivatives since π-donation destabilizes $M(PMe_3)_4X_2$ by raising the energy of the antibonding HOMO. The distinction with the Vaska system arises from the fact that the d_{xz} and d_{yz} orbitals in $M(PMe_3)_4X_2$ are degenerate and interact with a *pair* of halogen p_π orbitals. As a result, $p_\pi - d_\pi$, donation destabilizes $M(PMe_3)_4X_2$ due to "filled−filled" repulsions. In contrast, symmetry considerations do not dictate that both halogen lone pairs in *trans*-$Ir(PPh_3)_2(CO)X$ must interact in a pairwise fashion with the iridium orbitals, and, as a consequence, π-donation of a single halogen lone pair may *stabilize* the system. The significant differences between $M(PMe_3)_4X_2$ and $Ir(PPh_3)_2(CO)X$ toward oxidative addition of H_2 provide an important example which indicates that ancillary ligand variations may not necessarily exert the same influence on a given reaction in different systems.

Equilibrium studies of the reaction of H_2 with $W(PMe_3)_4I_2$ indicate that the oxidative addition is characterized by an *inverse* equilibrium deuterium isotope effect [$K_H/K_D = 0.63(5)$ at 60 °C]. The inverse nature of the equilibrium isotope effect is associated with the large number (six) of isotope-sensitive vibrational modes in the product, compared to the single isotope-sensitive vibrational mode in H_2.

Finally, a mechanistic study reveals that oxidative addition of H_2 does not proceed directly to $M(PMe_3)_4I_2$. Rather, the reaction proceeds via initial dissociation of PMe_3 and oxidative addition to five-coordinate $[W(PMe_3)_3I_2]$. Conversely, reductive elimination of H_2 does not occur directly from $W(PMe_3)_4H_2I_2$ but rather by a sequence that involves dissociation of PMe_3 and reductive elimination from seven-coordinate $[W(PMe_3)_3H_2I_2]$.

Experimental Section

General Considerations. All manipulations were performed using a combination of glovebox, high-vacuum, and Schlenk techniques.[91] Solvents were purified and degassed by standard procedures. NMR spectra were measured on Varian VXR 200, 300, and 400 spectrometers and Bruker Avance DRX300WB and Bruker DPX300 spectrometers. ^{31}P NMR spectra are referenced relative to 85% H_3PO_4 ($\delta = 0$) using $P(OMe)_3$ as an external reference ($\delta = 141.0$); all "*J*" values are given in hertz. $Mo(PMe_3)_5H_2$,[92] $Mo(PMe_3)_4H_2F_2$,[9] and $W(PMe_3)_4H_2I_2$[4] were prepared as previously reported.

Synthesis of $Mo(PMe_3)_4H_2Cl_2$. A solution of $Mo(PMe_3)_5H_2$ (0.48 g, 1.00 mmol) in pentane (30 mL) was treated dropwise with HCl_{aq} (12 M), giving a yellow precipitate. The addition was continued until no further precipitation occurred (ca. 0.2 mL). The solid was isolated by filtration, washed with pentane (10 mL), and dried in vacuo overnight. Yield of $Mo(PMe_3)_4H_2Cl_2$: 0.36 g (76%). IR data (cm^{-1}): 2971 (m), 2904 (m), 1897 (w) [ν_{Mo-H}], 1423 (m), 1297 (m), 1280 (m), 940 (s), 846 (m), 716 (m), 665 (m). ^1H NMR data (C_6D_6): δ 1.30 [18 H, vt, "J_{P-H}" = 3, 2 PMe_3], 1.24 [18 H, vt, "J_{P-H}" = 3, 2 PMe_3], −5.85 [2 H, d, $^2J_{P-H} = 42$: d, $^2J_{P-H} = 47$; t, $^2J_{P-H} = 72$, MoH_2]. ^{13}C NMR (C_6D_6): δ 25.6 [vt, "J_{P-C}" = 14; q, $^1J_{C-H} = 128$, 2 PMe_3], 19.2 [vt, "J_{P-C}" = 11; q, $^1J_{C-H} = 127$; $^1J_{C-H} = 129$, 2 PMe_3]. ^{31}P NMR data (C_6D_6): δ 13.8 [$J_{P-P} = 25$, 2 PMe_3], −8.3 [t, $^2J_{P-P} = 25$, 2 PMe_3].

Synthesis of $Mo(PMe_3)_4H_2Br_2$. A solution of $Mo(PMe_3)_5H_2$ (0.38 g, 0.79 mmol) in pentane (20 mL) was treated with HBr (48% aqueous) in a dropwise manner, resulting in the formation of a yellow precipitate. The addition was continued until no further precipitation was observed (ca. 0.3 mL). The mixture was filtered, and the solid was washed with pentane (10 mL) and dried in vacuo overnight. Yield of $Mo(PMe_3)_4H_2Br_2$: 0.35g (79%). IR data (cm^{-1}): 2971 (m), 2903 (m), 1907 (w) [ν_{Mo-H}], 1422 (m), 1280 (m), 939 (s), 845 (m), 779 (w), 714 (m), 664 (m). ^1H NMR data (C_6D_6): δ 1.38 [18 H, vt, "J_{P-H}" = 3, 2 PMe_3], 1.26 [18 H, vt, "J_{P-H}" = 4, 2 PMe_3], −6.91 [2 H, t, $^2J_{P-H} = 45$; t, $^2J_{P-H} = 72$, MoH_2]. ^{31}P NMR data (C_6D_6): δ 7.0 [t, $^2J_{P-P} = 26$, 2 PMe_3], −17.8 [t, $^2J_{P-P} = 26$, 2 PMe_3].

Synthesis of $Mo(PMe_3)_4I_2$. A solution of $Mo(PMe_3)_5H_2$ (2.0 g, 4.2 mmol) in pentane (150 mL) was treated with HI_{aq} (57 wt %) in a dropwise manner, resulting in the formation of a tan precipitate. The addition was continued until no further precipitation was observed. The mixture was filtered, and the solid was dried in vacuo, extracted into

(90) Earlier theoretical studies calculated that the kinetic isotope should be inverse on the basis of the MMI, EXC, and EXP(ZPE) terms (ca. 0.5) and therefore introduced a tunneling correction to achieve a normal kinetic isotope effect.[a] The more recent study, however, indicates that tunneling is not a required correction.[b] (a) Zhou, P.; Vitale, A. A.; San Filippo, J., Jr.; Saunders, W. H., Jr. *J. Am. Chem. Soc.* **1985**, *107*, 8049−8054. (b) Reference 41b.

(91) (a) McNally, J. P.; Leong, V. S.; Cooper, N. J. In *Experimental Organometallic Chemistry*; Wayda, A. L., Darensbourg, M. Y., Eds.; American Chemical Society: Washington, DC, 1987; chapter 2, pp 6-23. (b) Burger, B. J.; Bercaw, J. E. In *Experimental Organometallic Chemistry*; Wayda, A. L., Darensbourg, M. Y., Eds.; American Chemical Society: Washington, DC, 1987; Chapter 4, pp 79−98.

(92) Lyons, D.; Wilkinson, G.; Thornton-Pett, M.; Hursthouse, M. B. *J. Chem. Soc., Dalton Trans.* **1984**, 695−700.

hot toluene (50 mL), and filtered. The filtrate was allowed to cool to room temperature, depositing a red microcrystalline solid which was isolated by filtration, washed with pentane (5 mL), and dried in vacuo. Yield of $Mo(PMe_3)_4I_2$: 1.30 g (48%).

Stability of $Mo(PMe_3)_4H_2F_2$ with Respect to H_2 Loss. A solution of $Mo(PMe_3)_4H_2F_2$ (ca. 15 mg) in C_6D_6 (0.7 mL) was heated at 30 °C for 2 days. The mixture was monitored by ^{1}H NMR spectroscopy, which indicated that $Mo(PMe_3)_4H_2F_2$ was stable to loss of H_2 under these conditions.

Interconversion of $Mo(PMe_3)_4H_2Cl_2$ and $Mo(PMe_3)_4Cl_2$. (a) A solution of $Mo(PMe_3)_4H_2Cl_2$ (ca. 15 mg) in C_6D_6 (0.7 mL) was heated at 60 °C for 5 min. The complete conversion to $Mo(PMe_3)_4Cl_2$ was demonstrated by ^{1}H NMR spectroscopy. At 30 °C, the half-life is ca. 2 h.

(b) A solution of $Mo(PMe_3)_4Cl_2$ (ca. 15 mg) in C_6D_6 (0.7 mL) was treated with H_2 (1 atm) and heated at 60 °C for 4 days. The mixture was monitored by ^{1}H NMR spectroscopy, which indicated that $Mo(PMe_3)_4Cl_2$ was stable with respect to $Mo(PMe_3)_4H_2Cl_2$ under these conditions.

Conversion of $Mo(PMe_3)_4H_2Br_2$ to $Mo(PMe_3)_4Br_2$. (a) A solution of $Mo(PMe_3)_4H_2Br_2$ (ca. 15 mg) in C_6D_6 (0.7 mL) was heated at 30 °C for 3 h. The complete conversion to $Mo(PMe_3)_4Br_2$ over this period was demonstrated by ^{1}H NMR spectroscopy ($t_{1/2} < 30$ min).

(b) A solution of $Mo(PMe_3)_4Br_2$ (ca. 10 mg) in C_6D_6 (0.7 mL) was treated with H_2 (1 atm) and heated at 55 °C for 3 h. The mixture was monitored by ^{1}H NMR spectroscopy, which indicated that $Mo(PMe_3)_4Br_2$ was stable with respect to $Mo(PMe_3)_4H_2Br_2$ under these conditions.

Stability of $Mo(PMe_3)_4I_2$ with Respect to Addition of H_2. A solution of $Mo(PMe_3)_4I_2$ (ca. 10 mg) in C_6D_6 (0.7 mL) was treated with H_2 (1 atm) and heated at 80 °C for 4 days. The mixture was monitored by ^{1}H NMR spectroscopy, which indicated that $Mo(PMe_3)_4I_2$ was stable with respect to $Mo(PMe_3)_4H_2I_2$ under these conditions.

Thermodynamics and Kinetics of the Equilibration of $W(PMe_3)_4I_2$ and H_2 with $W(PMe_3)_4H_2I_2$. (a) Equilibrium Studies. In a typical experiment, a solution of $W(PMe_3)_4H_2I_2$ in C_6D_6 (0.8 mL of 10.1 mM) in a gas-tight NMR tube was saturated with H_2 (1 atm at 23 °C). The sample was placed in a constant temperature oil bath (± 1 °C) and removed periodically to monitor (by ^{1}H NMR spectroscopy) the formation of the equilibrium mixture with $W(PMe_3)_4I_2$. The molar ratio of $W(PMe_3)_4H_2I_2$ to $W(PMe_3)_4I_2$ was determined directly from the ^{1}H NMR spectra, and the molar concentration of dihydrogen in solution at equilibrium was estimated by a method similar to that described previously,[93] using a combination of Henry's law with the mole fraction solubilities of H_2 calculated directly or extrapolated from the equation given by Clever.[94] The equilibrium constant (K) was measured over the temperature range 40−90 °C (Table 2), and a van't Hoff plot of ln K vs $1/T$ (Figure 1) yielded the values $\Delta H°$ and $\Delta S°$ from the slope and the intercept of the resulting straight line, respectively. An analogous procedure was used for the equilibrium studies between $W(PMe_3)_4I_2$ and $W(PMe_3)_4D_2I_2$, for which the mole fraction solubilities of D_2 were calculated directly or extrapolated from the equation given by Clever.[95]

(b) Kinetics Studies. Samples of $W(PMe_3)_4I_2$ for kinetics studies at 60 °C were prepared by a method analogous to that described above, but variable amounts of PMe_3 were added prior to saturation with H_2 at 23 °C. The concentration of H_2 at 60 °C was determined as described above, while the concentration of PMe_3 was determined by integration with respect to mesitylene as an internal standard. Samples of $W(PMe_3)_4H_2I_2$ were prepared similarly, except H_2 was not added. The result of application of the steady-state approximation for the intermediates $[W(PMe_3)_3I_2]$ and $[W(PMe_3)_3H_2I_2]$ for the mechanism of Scheme 2 is given in Chart 1 in the Supporting Information. For convenience, the kinetics were analyzed by separately examining the oxidative addition and reductive elimination reactions using the method of initial rates. The pseudo-first-order rate constants, k_{oa} and k_{re}, as a function of PMe_3 concentration are listed in Tables S7 and S8 in the Supporting Information. For the reductive elimination reaction, a plot of $1/k_{re}$ versus $[PMe_3]$ (Figure 11) allows k_3 to be established from the intercept, since $[H_2] = 0$ during the initial stages of the reaction. The ratio k_{-2}/k_3 may likewise be determined from the slope, using the aforementioned value of k_{-3}. For the oxidative addition reaction, a plot of $1/k_{oa}$ versus $[PMe_3]$ (Figure 11) allows k_1 to be determined from the intercept, since k_{-3}, K, and $[H_2]$ are known. Correspondingly, the ratio k_{-1}/k_2 may be determined from the slope, since k_i and $[H_2]$ are known. $\Delta G^‡$ was calculated from the Eyring equation, $\Delta G^‡ = RT \ln(\kappa k_B T/kh)$, assuming a transmission coefficient (κ) of 1.

Computational Details. All DFT calculations were performed using Jaguar Version 3.5. Geometries were optimized at the BLYP level using the LACVP** basis set. D_{2d} symmetry and triplet multiplicity were used for the $M(PR_3)_4X_2$ (R = H, Me; X = F, Cl, Br, I) complexes; C_{2v} symmetry and singlet multiplicity were used for $M(PH_3)_4H_2X_2$ complexes; C_s symmetry and singlet multiplicity were used for $M(PMe_3)_4H_2X_2$ complexes.[96] For $W(PMe_3)_4(NH_2)_2$, the structure was optimized using both singlet and triplet multiplicities. The singlet refinement converged to a structure with parallel NH_2 groups and C_{2v} symmetry, while the triplet refinement converged to a structure with orthogonal NH_2 groups and D_{2d} symmetry. For $W(PMe_3)_4H_2(NH_2)_2$, the structure was optimized with singlet multiplicity and no symmetry constraints. Single-point energies were then calculated on all optimized structures (with appropriate symmetry constraints) at the B3LYP level using triple-ζ basis sets (LACV3P** for Mo, W, Br, and I and cc-pvtz(-f) for all other elements). H_2 was optimized at the B3LYP level using the cc-pvtz(-f) basis set, giving a calculated bond length of 0.74 Å.

Comparisons of experimental and calculated structural parameters for the compounds studied are presented in Tables S2−S5 in the Supporting Information. In general, the angular values obtained from the DFT calculations agree quite well with those determined via crystallography. However, there are substantial and systematic differences that can be observed for some of the bond lengths. In particular, the metal−halide and metal−phosphorus bond lengths are systematically overestimated. In the most extreme cases, for example the iodide species, the deviations would appear to be outside of the range normally expected for DFT calculations as compared to experiment, even for metal-containing systems, based on the data available in the literature.[97]

We have investigated this issue in detail as follows. First, we ran calculations using the fully analytical integral (as opposed to pseudospectral) methodology available in Jaguar for the entire series of six-coordinate complexes $M(PMe_3)_4X_2$ (M = Mo, W; X = F, Cl, Br, I), as illustrated in Table S9 of the Supporting Information. For all test cases, differences in bond lengths between pseudospectral and analytical results were less than 0.005 Å when the default DFT grid was used. Use of a fine DFT grid in the analytical calculations resulted in little change. Second, we carried out calculations on $W(PMe_3)_4H_2I_2$ using a hybrid functional incorporating exact HF exchange (B3LYP) rather than the BLYP functional that was used as a standard for the geometry optimizations in the present work. This produced a small improvement, but on the scale of the deviation from experiment, the change was not significant—a rather surprising result as gradient-corrected and hybrid functionals often give structures with significant differences. Finally, we ran an LMP2 rather than DFT geometry optimization for $W(PMe_3)_4H_2I_2$. The LMP2 results are closer to the experimental results than are the DFT results but still differ from them significantly.[98]

In addition, the series of Mo complexes $Mo(PH_3)_4X_2$ and $Mo(PH_3)_4H_2X_2$ (X = F, Cl, Br, I) were optimized at the B3LYP level using the LACVP** basis set, and then single-point energy calculations were performed on the optimized structures using triple-ζ basis sets as described above. This procedure resulted in minor differences in the Mo−X bond lengths, as shown in Table S10 of the Supporting Information. Of more importance to the present study, it can be seen

(93) Thompson, M. E.; Baxter, S. M.; Bulls, A. R.; Burger, B. J.; Nolan, M. C.; Santarsiero, B. D.; Schaefer, W. P.; Bercaw, J. E. *J. Am. Chem. Soc.* **1987**, *109*, 203−219.

(94) $\ln x = -5.5284 - 813.90/(T/K)$. See: Clever, H. L. Hydrogen and Deuterium. In *Solubility Data Series*, Young, C. L., Ed.; Pergamon Press: Oxford, 1981; Volume 5/6, p 159.

(95) $\ln x = -5.7399 - 743.44/(T/K)$. See: Clever, H. L. Hydrogen and Deuterium. In *Solubility Data Series*, Young, C. L., Ed.; Pergamon Press: Oxford, 1981; Volume 5/6, p 287.

(96) Crystallographic studies indicate that $M(PMe_3)_4H_2X_2$ complexes exist as several rotamers in the solid state, depending upon the orientation of the PMe_3 methyl groups. For consistency, all calculations were performed for a common rotameric structure.

(97) Frenking, G.; Pidun, U. *J. Chem. Soc., Dalton Trans.* **1997**, 1653−1662.

(98) W−I bond lengths (Å): BLYP, 3.040, 3.106; B3LYP, 3.014, 3.067; LMP2, 3.003, 3.037; expt, 2.903, 2.922.

that performing the geometry optimizations at the B3LYP level has a negligible effect on the calculated energies for the addition of H_2 to $Mo(PH_3)_4X_2$ (Table S11 of the Supporting Information).

The sum total of the results suggests that the deviations in bond length are, in fact, a consequence of the DFT treatment of electron correlation for this particular system, which appears to be considerably more challenging than other, simpler, transition metal systems for which results have been reported in the literature. It is also possible that there is some contribution to the deviation from crystal packing effects (not modeled in our calculations), but the magnitude of the deviation is larger than can plausibly be explained by this. Clearly, this problem warrants further investigations, using higher levels of electron correlation such as multireference perturbation theory, and we intend to pursue such calculations in future work. For the present paper, however, the observed deviations in bond length from the experimental data are not incompatible with reasonable predictions for bond energies or other relative properties of the various molecules, and we judge that the calculations are still quite useful in this regard.

Acknowledgment. G.P. thanks the U.S. Department of Energy, Office of Basic Energy Sciences (DE-FG02-93ER14339), for support of this research. This work was also supported in part by a grant to R.A.F. from the NIH (GM-40526). Dr. Bruce Bender is gratefully thanked for providing us with a copy of his program to calculate MMI, EXC, and ZPE terms.

Supporting Information Available: Tables S1-S11 of selected W−H bond energies, comparisons of calculated and experimentally determined structures, a compilation of mechanisms for oxidative addition and reductive elimination reactions, and experimentally determined rate constants for oxidative addition of H_2 to $W(PMe_3)_4I_2$ and for reductive elimination of H_2 from $W(PMe_3)_4I_2H_2$; Chart 1, giving kinetic expressions for oxidative addition of H_2 to $W(PMe_3)_4I_2$ and for reductive elimination of H_2 from $W(PMe_3)_4I_2H_2$ (PDF). This material is available free of charge via the Internet at http://pubs.acs.org.

JA9920009